Palaeontology
The Palaeontological Association
www.palass.org
[Palaeontology, Vol. 67, Part 4, 2024, e12720]

Morphological disparity of mammalian limb bones throughout the Cenozoic: the role of biotic and abiotic factors

by CARMELA SERIO[1]*, RICHARD P. BROWN[1], MARCUS CLAUSS[2] *and* CARLO MELORO[1]

[1]Research Centre in Evolutionary Anthropology and Palaeoecology, School of Natural Sciences and Psychology, Liverpool John Moores University, 3 Byrom St, L3 3AF Liverpool, UK; karmserio@gmail.com, r.p.brown@ljmu.ac.uk, c.meloro@ljmu.ac.uk
[2]Clinic for Zoo Animals, Exotic Pets and Wildlife, Vetsuisse Faculty, University of Zurich, Winterthurerstr. 260, 8057 Zurich, Switzerland; mclauss@vetclinics.uzh.ch
*Corresponding author

Typescript received 3 November 2023; accepted in revised form 16 July 2024

Abstract: Mammals exhibit ecology-related diversity in long bone morphology, revealing an ample spectrum of adaptations both within and between clades. Their occupation of unique ecological niches in postcranial morphology is thought to have occurred at different chronological phases in relation to abiotic factors such as climate and biotic interactions amongst major clades. Mammalian morphologies rapidly evolved throughout the Cenozoic, with several orders following different paths in locomotory adaptations. We assessed morphological variation in limb proportions for a rich sample of extant and fossil large mammalian clades (mainly carnivores and ungulates) to test associations with ecological adaptations and to identify temporal patterns of diversification. Phylogenetic relationships among species were incorporated into the analysis of limb bone proportions, showing significant morphological changes in relation to species substrate preference. Major climatic events appeared to have no temporal impact on patterns of morphological diversification, expressed as morphological disparity, in either clades or ecological groups. Linear stochastic differential equations supported a double-wedge diversification model for limb proportions of carnivorous clades ('Creodonta' and Carnivora). The concomitant increase in morphological disparity throughout the Cenozoic for the orders Carnivora and Artiodactyla had a significative impact on the disparity of Perissodactyla supporting biotic interaction as primary driver of mammalian morphological diversification. Our findings challenge the classic idea of abiotic factors as primary driving forces in the evolution of postcranial morphologies for large terrestrial mammals, and propose clade competition as a key factor in temporal diversification.

Key words: disparity, limb ratio, mammal, ecological adaptation, clade interactions.

MAMMALS appeared during the Mesozoic era when dinosaurs were the predominant terrestrial vertebrates. Mesozoic mammals were thought to be small fossorial and arboreal species that occupied ecological niches similar to small-sized (<1 kg) living taxa (Osborn 1902; Kielan-Jaworowska *et al.* 2004; Archibald 2011). However, it has recently been discovered that stem mammals were ecologically diverse in size, diet and locomotion (Chen & Wilson 2015; Benevento *et al.* 2019; Grossnickle *et al.* 2019; Morales-García *et al.* 2021). The fifth mass extinction at the end of the Mesozoic (*c.* 66 Ma) impacted many species, including non-avian dinosaurs, and opened new ecological opportunities for mammals (Clemens 2002; Archibald 2011).

Simpson (1944) described three different modes by which organisms diversify to occupy new niches: (1) the emergence of a key innovation; (2) the niches emptying due to competitor extinction; and (3) the emergence of a new niche. Starting from the Mesozoic, mammals diversified according to all of these models from primitive and archaic morphotypes into more diverse and specialized forms (Figueirido *et al.* 2019; Shelley *et al.* 2021). Such diversification of mammalian body plans has been generally accompanied by shifts in rates of body size evolution coupled by modification in body proportions, particularly of the postcranial skeleton. Mesozoic taxa had more robust limb morphologies than Cenozoic species (Shelley *et al.* 2021) possibly because mammals were quite constrained in their realized ecological niche. A similar observation has been made for body size with a release in mammalian body size evolution after the K–Pg extinction (Slater 2013). Mammals with robust limbs survived until the Paleocene–Eocene Thermal Maximum (66–33.9 Ma) when there were global reductions in tropical forests and

doi: 10.1111/pala.12720

new and diverse habitats emerged (Shelley *et al.* 2021). Studies on body size have found significant increases in mammalian variation at this time (Slater 2013).

If mammalian morphologies were well established by the beginning of the Cenozoic, the evolution of different mammalian orders followed quite different paths, especially in relation to extreme locomotory adaptations. One example was identified by Janis & Wilhelm (1993) who examined the evolution of limb proportions in clades of mammalian predators (i.e. the Carnivora and 'Creodonta') and their ungulate prey (including terrestrial even-toed Artiodactyla, and odd-toed Perissodactyla). During the Palaeogene, Hyaenodonta and Oxyaenida, grouped in the possibly paraphyletic 'Creodonta' (Zack 2019), were the dominant predator groups, and their extinction coincided with an increase in the Carnivora diversification. Even if Hyaenodonta, Oxyaenodonta and Carnivora occupied similar trophic niches, it is unclear whether competition was the cause of the former extinction (Friscia & Van Valkenburgh 2010; Christison *et al.* 2022). Nonetheless, modern ungulates appeared in the Eocene, probably in Eurasia, and then migrated to North America (Gingerich 2006; Gould 2017). Early ungulates were small body-sized species adapted to folivorous or frugivorous diets (Saarinen *et al.* 2020). Species with larger body sizes and longer legs appeared following the emergence of grassland (Garland & Janis 1993; Janis & Wilhelm 1993), but the evolution of specialized grazers occurred only after an extension of open habitats (Janis 2008; Saarinen *et al.* 2020). In North American Artiodactyla and Perissodactyla, Morales-García *et al.* (2020) observed an increase in morphological diversity during the Middle Miocene Climatic Optimum followed by a decline toward the present. Artiodactyla and Perissodactyla have shared similar ecosystems since their origins. Perissodactyla were more diverse throughout the Palaeogene than Artiodactyla, which became the dominant ungulates during the Neogene. Despite the biological similarities between even and odd toed mammals, this turnover was assumed to be influenced by climatic change in the Cenozoic (Janis 1989).

Climate-related changes in mammalian limb bones have also been the focus of several studies. Lovegrove & Haines (2004) suggested that the emergence of grassland triggered the evolution of cursorial mammals. When this open habitat appeared, carnivores and ungulates shifted from the plesiomorphic plantigrade foot to digitigrade and unguligrade stances. The new cursorial morphotypes, including long vertically oriented limbs with relatively short stylopodia (humerus and femur) as compared to zeugopodia (radius–ulna and tibia–fibula) and autopods (metacarpal and metatarsal; Janis & Wilhelm 1993; Levering *et al.* 2017), allowed greater locomotor performance (Lovegrove 2004).

The relative proportions of the zeugopodia and stylopodia can be used to estimate the maximum running speed in fossil species (Christiansen 2002). Specifically, the radius to humerus ratio (R/H), known also as the brachial index, has been identified as the best proxy for running speed in large mammals. While less effective, the tibia to femur ratio (T/F), known as crural index, has also been shown to significantly predict maximum running speed (Christiansen 2002). In both cases, higher ratios (i.e. longer zeugopodia than stylopodia) are associated with increased speed. These strong associations with limb ratios provide the basis for inferring changes in locomotor performance of terrestrial mammals.

Recent analysis of North American ungulates has proposed a link between climate change and the diversification of limb bone proportions (Levering *et al.* 2017). Similarly, Figueirido *et al.* (2015), found an association between climate and limb evolution in North American canids, associated with behavioural changes in hunting mode, while analyses of extant Carnivora have revealed a significant relationship between the brachial index and average precipitation (Meachen *et al.* 2016). The evolution of long limbs, first in ungulates and 20 million years later in carnivores (Garland 1983; Janis & Wilhelm 1993), has been suggested as the most important evolutionary 'arms race' that occurred in mammals, possibly accompanied by a streamlining of the torso for optimal maneuverability of the respective trophic groups (Clauss *et al.* 2017). However, other authors have rejected the 'arms race' hypothesis, instead proposing the optimization of the cost of transport for finding food (Garland & Janis 1993; Pontzer & Kamilar 2009; Levering *et al.* 2017) or the emergence of grazing in ungulates (Lovegrove & Mowoe 2013) as driving factors for the evolution of mammalian long bones. According to Lovegrove & Mowoe (2013), the grazing diet drove the evolution of larger body size in unguligrade to optimize cellulose digestion, followed by limb elongation due to body mass increase.

Other ecological factors could also potentially explain the evolution of mammalian limb bone morphologies. Substrate preference and habitat type have been found to influence size and shape of long bones in several orders, such as Xenarthra, Rodentia, Carnivora, ungulates and Primates (Elton 2001, 2002, 2006; Carrizo *et al.* 2014; Schellhorn & Pfretzschner 2015; Serio *et al.* 2020; Etienne *et al.* 2021; Toledo *et al.* 2021) although no convergent traits could be identified between disparate groups (i.e. primates, bovids, suids and felids; Elton *et al.* 2016). This suggests that each separate mammalian order may occupy a distinct ecomorphological niche in limb proportions, although this remains to be demonstrated.

We hypothesize that ecological variables such as diet, substrate preferences or trophic level continue to play an important role in the evolution of limb proportions

especially in large mammalian clades, regardless of their phylogenetic relationships. Additionally, we predict the occupation by mammals of different ecological niches in relation to different post-cranial morphologies to have possibly occurred at different times due to climate change or biotic interaction among the major clades. To test these hypotheses, we assembled a database of brachial and crural indices, covering the main groups of carnivores and unguligrade mammals of the Cenozoic, and implemented comparative analyses within a phylogenetic framework. The impact of biotic or abiotic factors on the temporal diversification of mammalian limb proportions was assessed by exploring patterns of morphological disparity through time. Disparity is a metric commonly used to quantify variation in morphological traits across clades and temporal intervals (Foote 1997; Guillerme *et al.* 2020). Previous research on different vertebrate clades showed that morphological disparities vary drastically among groups and across time (Brusatte *et al.* 2008; Prentice *et al.* 2011; Ruta *et al.* 2013; Schaeffer *et al.* 2020; Reeves *et al.* 2021; Stubbs *et al.* 2021; Cross *et al.* 2022).

The link between climate and morphological disparity is likely to vary within the interacting predatory carnivores and ungulates clades over evolutionary time (Cross *et al.* 2022). Due to the different timing of cursorial adaptations recognized in large predatory carnivores and large prey ungulates (Janis & Wilhelm 1993), the link between climate and morphological disparity is likely to vary across these clades (Cross *et al.* 2022). In that case, we predict a variation in morphological disparity in association with the Cenozoic climatic change events.

Alternatively, we hypothesized that biotic interactions had a primary influence on the evolution of mammalian limb proportions, so that morphological disparities should be significantly correlated between clades (negatively if clade replacement or competition occurred; Benton 2009). We used the linear stochastic differential equations (SDE; Oksendal 2013) as implemented by Reitan & Liow (2019) to account for temporal autocorrelation in disparity and climate data. As illustrated by Lidgard *et al.* (2021), this method may be used to successfully establish causation in palaeontological data by analysing species diversity across time.

MATERIAL AND METHOD

Data collection

A total of 793 humeral, 805 radial, 668 femoral, and 663 tibial lengths were assembled from the literature and published databases (Serio *et al.* 2024, data 1). These data were combined into the two functional radius to humerus (R/H; i.e. the brachial index) and tibia to femur (T/F; i.e. the crural index) ratios. We also assembled a large database including 1883 greatest skull length values (GSL; Serio *et al.* 2024, data 1). This variable is strongly related to general species size and can be successfully employed to predict body mass in fossil mammals (Damuth & MacFadden 1990). GSL was used to account for the allometric effect on limb proportions in the statistical analyses. On average, data for each species were assembled by merging multiple individual references. The final dataset included all values for 420 (173 fossils and 247 living) terrestrial mammals from the orders Acreodi (1), Artiodactyla (179), Carnivora (168), Cimolesta (4), Condylarthra (3), Hyaenodonta (5), Oxyaenodonta (4), Dinocerata (1), Perissodactyla (53) and Procreodi (2) living throughout the Cenozoic. Despite being classified as distinct orders, the Hyaenodonta and Oxyaenodonta were grouped into 'Creodonta' due to the small sample size and their functional similarities in dental formula and locomotory mode when compared to Carnivora.

Here, we will use the term 'ungulates' to refer to the polyphyletic unranked group including terrestrial Artiodactyla, Perissodactyla, Condylarthra and Dinocerata, and the term 'carnivores' to refer to the group including Carnivora, 'Creodonta', Cimolesta, Acreodi and Procreodi. Data were checked for errors due to the merging of multiple sources (see Appendix S1). All data were $\log_{10}$ transformed before the analyses.

Phylogenetic tree

To account for shared evolutionary history, we used four different backbone topologies to assemble a large informal phylogenetic tree which included 247 living and 173 fossil species (Cerdeño 1996; Nyakatura & Bininda-Emonds 2012; Cantalapiedra *et al.* 2017; Zurano *et al.* 2019; Álvarez-Carretero *et al.* 2021). Details about the phylogenetic position of each species with the relative scientific references are provided in Serio *et al.* (2024, data 2). More specific details regarding phylogenetic tree topology are discussed in Appendix S1.

To calibrate the informal supertree, species last occurrences (LDA) were compiled from the Fossilworks database (http://www.fossilworks.org; Serio *et al.* 2024, data 2) and data for internal node ages were collected from the literature (Serio *et al.* 2024, data 3). Tip and node ages (i.e. time distance of each tip and node from the recent) were used to assign branch lengths for the entire phylogeny. Fossil species were designated to become extinct at the age of their last occurrence in the fossil record, whereas living species had an age of zero. We used *tree.merger* to merge the backbone trees, add missing species (or a whole clade), and calibrate the final supertree, (R package RRPhylo; Castiglione *et al.* 2022).

The resulting phylogeny was employed to apply phylogenetic comparative methods and to include the reconstructed ancestral states in the computation of morphological disparity through time (Brusatte *et al.* 2011). This procedure has proved effective for several vertebrate clades (archosaurs, crocodyliformes, Carnivoramorpha, Eurypterida, Captorhinidae and euarchontoglirans; Brusatte *et al.* 2011; Brocklehurst 2017; Lamsdell & Selden 2017; Wilberg 2017).

Ecological categories

A database was constructed containing information about trophic level, diet and substrate preferences, for both extant and extinct species (Serio *et al.* 2024, data 2), to help determine the selective pressures that were associated with the limb ratios.

Trophic level categories were created to investigate how the functional morphospace was partitioned, assuming that the predator/prey relationship was a strong selective force with respect to relative limb proportions (Table 1; Janis & Wilhelm 1993). The large predator category was based on Carbone *et al.* (1999) and included carnivorous species weighing more than 21.5 kg and capable of killing ungulates larger than themselves, even though we are aware that large and small prey feeders may occur across the whole body mass range of carnivores (De Cuyper *et al.* 2019). Large carnivores are thought to have the greatest impact on prey biomass and ecosystem functioning (Hoeks *et al.* 2020). Amphicyonids, nimravids, barbourofelids, machairodonts and arctocyonids are examples of fossil taxa in this category. The small predator category included carnivores <21.5 kg specialized on small vertebrates (i.e. small birds or lizards) and invertebrates (Carbone *et al.* 1999; Carbone *et al.* 2007). Examples of fossil taxa included in this category are the canids *Desmocyon*, *Cormocyon*, *Phlaocyon* and *Archaeocyon* as well as *Eucyon*, *Limocyon*, *Thinocyon*, *Lesmesodon*, *Palaeonictis*, *Buxolestes*, *Paleosinopa* and *Chriacus*. The large prey category included all ungulates between 10 and 900 kg. Estes (1974) suggested that ungulates weighing up to 450 kg were key prey in savannah ecosystems and this also appears to be the case for ancient ecosystems (Meloro *et al.* 2007; Meloro & Clauss 2012). Analysis of food webs suggested that large predators generally have an impact on the biomass of all ungulates up to 900 kg as these can be easily preyed upon (Sunquist & Sunquist 1989; Owen-Smith & Mills 2008). Most of the species included in the large prey category belong to Perissodactyla and Artiodactyla including the fossil groups of phenacodontids, merycoidodonts, agriochoerids and uintatherids. Following Owen-Smith (1988), the megaherbivore category grouped all taxa over 900 kg. Due to their large body mass, these species were assumed to be virtually immune to predation, although they are critical for nutrient cycling within the ecosystem. Fossil species included in the megaherbivore category were *Palaeosyops*, *Parvicornus*, *Coelodonta*, *Stephanorhinus*, *Chilotherium*, *Teleoceras*, *Paraceratherium*, *Juxia*, *Amynodon*, *Chalicotherium* and *Moropus*. The small prey category included ungulates smaller than 10 kg (Carbone *et al.* 1999; Carbone *et al.* 2007). Ursids were merged into the non-specialized predator category because these members of the Carnivora did not show specific predatory behaviour (Martín-Serra *et al.* 2016). With the exception of *Ursus maritimus*, living ursids only hunt occasionally (Martín-Serra *et al.* 2016; Ferretti *et al.* 2020) while *U. maritimus* preys preferentially on seals (Iversen *et al.* 2013; Florko *et al.* 2021), a group not considered for this study due to its highly derived postcranial morphology. Ungulate meat constitutes less than 10% of the diet of all the other living bears in our dataset (Penteriani & Melletti 2020). Among fossil species, the database includes the majority of Pleistocene omnivorous/herbivorous taxa representative of the cave bear lineage with the only exception being *Arctodus simus*. This latter species was unlikely to be a specialized predator, but instead the largest omnivore that ever lived (Figueirido *et al.* 2010; Meloro 2011a). This approach assumed that neither living nor prehistoric bears had a significant impact on terrestrial large prey dynamics due to their omnivorous nature. The red panda (*Ailurus fulgens*) was also included in this category even though it is not an ursid as it is well-adapted to a mostly folivorous diet, similar to that of the unrelated giant panda *Ailuropoda melanoleuca* (Roka *et al.* 2021).

Diet categories were insectivore, carnivorous, omnivore, piscivore, frugivore, folivore, browser, grazer and mixed feeder. The insectivore category included species such as members of the Herpestidae family, the hyaena *Proteles cristatus* and the canid *Otocyon megalotis*, while most of the Carnivora, the extinct 'Creodonta' and *Pachyaena ossifraga*, that primarily feed on vertebrate food, were

TABLE 1. Ranges of body mass used to define the trophic levels.

Category	Number of species	Definitions
Non-specialized predator	13	–
Large prey	193	≥10 kg to <900 kg
Small prey	16	<10 kg
Large predator	56	≥21.5 kg
Small predator	114	<21.5 kg
Megaherbivore	28	≥900 kg

classified as carnivorous. The omnivore category included species with a generalist diet such as extinct entelodonts and *Chriacus*, extant suids and bears. The piscivore category included the members of the Pantolestidae family as well as otters. Species that feed mainly on fruits such as the kinkajou, *Potos flavus*, were assigned to the frugivore category. The non-ungulate herbivores *Coryphodon molestus*, *Ailurus fulgens*, *Ailuropoda melanoleuca* and *Tremarctos ornatus* were classified as folivores. The browser category included ungulates feeding on leaves such as *Uintatherium anceps*, the basal perissodactyls *Hyracotherium*, most rhinoceroses, and camelids. Living ungulates, such as horses, most cervids, and bovids that feed on grass were classified as grazers while the mixed-feeders category included species that forage on both leaves and grass. The extinct Merycoidodontidae, which lived before the Early Miocene, were classified as browsers, while species that lived from the middle Miocene forward were assigned to the grazer category (Mihlbachler & Solounias 2006).

Substrate preference defined amphibious, arboreal, terrestrial, scansorial, and semi-fossorial categories. The extinct *Miacis gracilis*, the extant viverrids and some procyonids and felids were included in the arboreal category while most of the carnivores and the ungulates were in the terrestrial category. Species that spend long periods close to bodies of water were classified as amphibious, such as the extant polar bear, otters, the hippopotamus, some tapirids, and the extinct *Teleoceras*, *Buxolestes*, *Palaeosinopa* and *Metamynodon*. Most felids, Mephitidae, Mustelidae and Procyonidae, and the extinct *Agriochoerus antiquus* and *Chriacus*, capable of climbing, were assigned to the scansorial category. There were some exceptions regarding *Meles meles*, *Mellivora capensis* and *Taxidea taxus*, which were classified as semi-fossorial. Both diet and substrate preferences categories were mainly collected from http://www.fossilworks.org/ and https://paleobiodb.org/ databases. The data were downloaded from the Paleobiology Database (PBDB) on March 2022, using the order names and the following parameters: time intervals = Upper Cretaceous and Holocene. Taxonomic occurrences of Carnivora, Artiodactyla, Perissodactyla, 'Creodonta', and Cimolesta were recorded in the PBDB (https://paleobiodb.org/).

Habitat preferences of living species (open, closed, mixed and wetland habitats) were collected from the IUCN red list of threatened species (https://www.iucnredlist.org/) and Animal Diversity Web (https://animaldiversity.org/; Serio *et al.* 2024, data 2). Habitat specialization in extinct taxa is generally predicted based on limb proportions (Meloro 2011b; Levering *et al.* 2017), and so was not used in tests of association to avoid circular reasoning. Ecological categories were employed in statistical models that aimed to test associations between ecological role, diet, substrate preference or habitat type and limb proportions.

Relationships between variables

The final dataset of phenotypic traits consisted of radius to humerus and tibia to femur ratios and GSL. The relationships between these continuous variables were analysed using phylogenetic generalized least squares regression (PGLS; Harris & Steudel 1997). The models R/H ~ GSL and T/F ~ GSL (where long bones were the dependent and GSL the independent variables) were tested using *pgls* (R package caper; Orme *et al.* 2018). In addition, we used PGLS also to test for the correlation of ecological categories with GSL, R/H and T/F (Barr & Scott 2014). All models were applied to living species only, and then to the whole dataset, to test if the correlation with allometric variation on limb proportions is consistent across datasets (Christiansen 2002).

The PGLS method incorporates the phylogeny as an error term by simultaneously estimating the lambda parameter (Pagel 1999) using maximum likelihood (ML). Lambda represents a multiplier used for branch length transformation to account for different degrees of phylogenetic signal: lambda = 1 equates to Brownian motion; lambda = 0 for a star phylogeny across which traits evolve independently (Revell 2010). PGLS lambda is less sensitive to type 1 errors as compared to other methods such as the phylogenetic independent contrast (PIC) and so was preferred here (Revell 2010). Analyses were performed both accounting for and omitting the phylogenetic effect. When accounting for the phylogeny, the function *pgls* optimizes the branch length transformation between bounds using maximum likelihood (ML) with the parameter lambda equal to ML. When omitting the phylogenetic effect, the function *pgls* performs an ordinary least squares (OLS) regression model. In this case the parameter lambda was set to 0.0001.

Size and phylogenetic corrected principal component analysis

We computed a principal component analysis (PCA) to obtain a functional morphospace including the largest (*Paraceratherium*) and the smallest (*Mustela*) species in our dataset (Carrano 1999). To account for both allometric and phylogenetic effects in the PCA computation, a size and phylogenetic corrected PCA (Phy–PCA) was computed (Revell 2009). Phy–PCA returns the first PC which is mostly independent of phylogeny using the correlation matrix (retrieved from the phylogenetic tree) and reduces type 1 errors (Revell 2009). To follow

Revell's procedure, the function *phyl.resid* was employed first (R package phytools v2.1-1; Revell 2012) using GSL (proxy for species body size) as the independent variable and both R/H and T/F as dependent variables. This function computes residuals from the models: R/H ~ GSL and T/F ~ GSL using a multiple generalized least square regression. The lambda value was estimated using maximum likelihood (Revell 2009). The function *phyl.pca* (phytools; Revell 2012) was then used on the computed residuals to perform the Phy–PCA and obtain evolutionary independent principal component vectors (PCs). Phy–PCA was computed for living species and for the whole dataset in order to investigate which ecological categories were associated with morphospace occupation.

To analyse the effect of ecological categories on limb proportions, we used the approach described by Adams & Collyer (2018) and Collyer & Adams (2020). First, we extracted the variance–covariance matrix from the phylogenetic tree using *corPagel* (R package ape; Paradis & Schliep 2019) and the parameters determined from the PCs best evolutionary models (see Ancestral character estimation, below). The variance–covariance matrix was then used as a covariate to account for the non-independence of data (the function's parameter 'iter' was set to 10 000 iterations) in the function *lm.rrpp* (RRPP package v2.0.0; Adams & Collyer 2018). To evaluate significant differences between pairs of group categories, we used the *pairwise* function (RRPP; Adams & Collyer 2018). In addition, because permutation ANOVA does not take the phylogeny into account, PGLS was employed as analogous to the phylogenetic ANOVA. To this aim, each PC axis was regressed against each category variable (Barr & Scott 2014).

Ancestral character estimation

To phylogenetically correct the morphological disparity computation and account for sample incompleteness within Cenozoic time bins, we estimated ancestral characters at tree nodes. The new values were treated as real taxa for computing morphological disparity (Brusatte *et al.* 2011). Maximum likelihood was used to estimate continuous ancestral traits within each node of the phylogeny, whereas the Monte Carlo Markov Chain (MCMC) approach was used to estimate discrete ancestral characters (Felsenstein 2012).

To compute the ancestral character estimates (ACEs) of continuous variables for correct calculation of morphological disparity through time, the best mode of evolution was first assessed for each PC vector computed for the whole dataset using *fitContinuous* (R package geiger v2.1-1; Pennell *et al.* 2014). This function allowed testing evolutionary models alternative to Brownian motion such as Ornstein–Uhlenbeck (OU), early burst, lambda, kappa and delta. Brownian motion represents a 'random walk' model assuming the trait evolves randomly with constant variance (Felsenstein 1973). The OU model assumes that the trait evolves toward a phenotypic optimum (Butler & King 2004). The early burst model (Harmon *et al.* 2010) incorporates exponential increases or decreases in evolutionary rates through time. Lambda, kappa and delta are Pagel's transformation models (Pagel 1999). Lambda was described in the previous section. Kappa is a speciational model (i.e. change in phenotype occurs at tree nodes). When kappa = 1, rates of character changes follow Brownian motion, reflecting gradualism. By contrast, character changes only occur at speciation when kappa = 0. Delta is a time-dependent model indicating rate variation in traits evolution. Delta <1 means the rate of evolution decreases through time, and delta >1 means the rate of evolution increases through time. Delta equal to 1 means the rate of evolution is constant as expected under Brownian motion.

All the fitted models were compared using the Akaike Information Criterion (AIC) computed following the formula AIC = 2K−2ln(L) where K is the number of independent variables and L is the likelihood which describes how well the model reproduces the data. The *fitContinuous* function returns, for each model tested, the AIC corrected for the sample size (AICc). The models with the lowest AICc and a ΔAIC of less than 2 were selected as the best models. The parameters of the resulting best model were used to rescale the phylogenetic tree by means of the function *rescale* (geiger R package; Pennell *et al.* 2014). The rescaled tree, used in the function *fastAnc* (Revell 2012), allowed us to estimate ACEs. To compute ACEs, *fastAnc* works by considering each internal node as a tree root and follows the independent contrasts algorithm (Felsenstein 1985) to reconstruct the node phenotype.

The best model of evolution for the whole-sample category variables was fitted using *fitDiscrete* (Yang 2006; Pennell *et al.* 2014) which compares the Brownian motion model with the early burst and Pagel's models. The best model for the ecological categories was selected by comparing the AICs and ΔAICs. Also in this case, the function *rescale* (geiger; Pennell *et al.* 2014) was employed to rescale the phylogenetic tree according to the estimated best model parameter. The tree was used to compute the ACEs for discrete variable at the internal nodes using the *ancThresh* function (phytools; Revell 2012). This function estimates character states at nodes using a Bayesian MCMC approach (Felsenstein 2012). It returns a matrix with posterior probabilities computed for each group category. For each node, we chose the category with the highest posterior probability.

Disparity analysis

Disparity through time is a metric that represents morphological variance among species within a specific time interval (Foote 1997; Guillerme *et al.* 2020). We computed morphological disparity throughout the Cenozoic stratigraphic time bins twice. First using only sampled values, corresponding to the tips of the phylogeny, and then including ACEs in the analyses.

In the analysis of tips, species were binned according to 22 Cenozoic stages spanning from 66 Ma to the present (Serio *et al.* 2024, data 4; Benevento *et al.* 2019; Reeves *et al.* 2021; Shelley *et al.* 2021). Paleocene stages were collapsed together because of a small number of sampled species. Geological dates were collected from the International Chronostratigraphic Chart (v2021/07; Cohen *et al.* 2013). From http://www.fossilworks.org/, https://paleobiodb.org/#/, and https://nowdatabase.org/, we collected species first (FAD) and last (LAD) appearance data (Serio *et al.* 2024, data 2).

For the analysis that included the ACEs, species were binned in 25 time intervals (Serio *et al.* 2024, data 5). Here, the first bin was representative of the Late Cretaceous. The greatest number of time bins was achieved because ACEs were treated as real taxa, and the earliest intervals were filled with them. For the same reason, the Paleocene, which was previously assumed to be a unique time interval, was divided into separate stages. Each ACE was binned in the same bin as its first sampled descendant following the conservative approach described by Brusatte *et al.* (2011).

Because of the unimodal distribution of PC scores, it was possible to study disparity using the sum of variance metric (Benevento *et al.* 2019). This metric captures the spread of the clade under study in space measuring dissimilarity among species morphologies relatively to the sample mean (Guillerme *et al.* 2020; Hopkins & Gerber 2021; Shelley *et al.* 2021). However, because this metric is more sensitive to the number of samples in each bin (Foote 1993), a partial rarefaction was used to overcome potential sampling bias using *boot.matrix* (R package disparity; Guillerme 2018) with 500 bootstrap replicates using the 'full method' (Guillerme 2018). During each replicate, the rarefaction number changes, and intervals with the lowest number of samples were not rarefied. Disparity through time was computed in R using the *dispRity* function (dispRity v1.8; Guillerme 2018).

Finally, to explore how ecological groups and orders contributed to the change in morphological disparity, we computed the partial disparity analysis (PDA) using *MDA* function (MATLAB package MDA; Navarro 2003). In this case, orders with fewer than three species (i.e. Dinocerata, Acreodi, Procreodi and Condylarthra) were merged into the 'basal orders' group. *MDA* uses the PC scores matrices, the species presence–absence through time, and species presence–absence by groups to identify groups that were responsible for an increase (or decrease) in disparity through time. The analyses were performed using 10 000 bootstrap replications and 95% bootstrap confidence intervals were obtained as suggested in Navarro (2003).

Effect of temperature, primary productivity, species interaction & competition

To test the effect of temperature (i.e. $\delta^{18}O$) and primary productivity (i.e. $\delta^{13}C$) on morphological disparity, we collected climatic data covering the latest 83 myr from Zachos *et al.* (2008). For each time bin, we computed variance, mean and median of the stable isotopes $\delta^{18}O$ and $\delta^{13}C$ and computed a PCA using the *princomp* function (R package stats v4.3.1; R Core Team 2023) to summarize and evaluate the fluctuations in temperature and primary productivity across time. These isotopic values are strongly correlated with each other and PCA allowed us to summarize variation into single and mutually interpretable vectors.

Due to the temporal autocorrelation that occurs in both isotopic and morphological disparity time series, we applied the linear stochastic differential equation (SDE) approach (Oksendal 2013), to test the hypothesis that environmental changes and/or clade interactions affected morphological variation in mammalian limb proportions throughout the Cenozoic. This method does not require equidistant time point sampling and it has recently been used in a Granger causality framework to assess causal links between two or more time series event data. The Granger causality in statistics establishes whether one temporal time series can be used to infer another. The SDE model is based on the differential equation:

$$dX(t) = -\alpha(X(t)-\mu)\,dt + \sigma dB(t) \quad (1)$$

where X(t) is the dependent variable changing according to the time (t; the independent variable); $-\alpha(X(t)-\mu)$ describes how X changes with time; and $\sigma dB(t)$ is the stochastic component. α measures the strength 'pushing' the dependent variable toward the μ, which is the average of the dependent variable, and σ is the standard deviation. When α, μ and σ are constant the equation represents an OU model.

Because our study aimed to investigate the causal connection or correlation between morphological disparity and climatic changes, we can include the effects of climate into the stochastic part of Equation 1, that is, incorporate the morphological disparity (MD) association with climate (C):

$$dMD(t) = -\alpha_{MD}(MD(t) - \mu_{MD} - \beta[C(t) - \mu_C)]\, dt + \sigma_{MD} dB_{MD}(t) \quad (2)$$

here β represents the strength of the causal connection (Reitan & Liow 2019). This equation allows us to compare different models for disparities and climate and choose the best one based on the model likelihood and model Bayesian posterior probabilities (Reitan & Liow 2019). More specifically we compared two models: (1) no connections between climate and disparities; and (2) causal connection from climate to disparities. Both models were fitted using the *layer.analyzer* function (layeranalyzer v0.1.1; Reitan & Liow 2019) and compared using the function *compare.layered* which returns both maximum likelihood and the percentage of posterior probability for each model (Reitan & Liow 2019). Here, we searched for a causal connection between climate and total disparity, substrate preference disparities and order disparities.

We also searched for a causal connection or correlation in between the partial disparity values of the orders. In this case, we used the function *traverse.connections.layered* (Reitan & Liow 2019) which is built around *compare.layered* and explores the connections between multiple time series. More specifically, we explored causal connections or correlations between Carnivora and Artiodactyla, Carnivora and Perissodactyla, Artiodactyla and Perissodactyla, and Carnivora and 'Creodonta' pairs. For each pair, *traverse.connections.layered* allowed us to fit five models:

1. No connections between the morphological disparity of two competing orders
2. Causal connection from Order 1 disparity to Order 2 disparity
3. Causal connection from Order 2 disparity to Order 1 disparity
4. Causal connections from Order 1 disparity to Order 2 disparity and from Order 2 disparity to Order 1 disparity (2-way feedback system)
5. Correlative connection between Order 1 disparity and Order 2 disparity.

Again, models were compared using the *compare.layered* function. Model likelihood and model Bayesian posterior probabilities were used to assess the likelihood model (Reitan & Liow 2019). The PDA was computed in MATLAB version R2019b, while all R analyses used R v4.3.1; (R Core Team 2023). A significance level of 0.05 was used throughout.

Phylogenetic uncertainly

We used the *swapOne* function (RRphylo v2.8.0; Raia *et al.* 2019) to validate our results in light of the phylogenetic uncertainty. This function allows for a change in the position of the tree tips at random, altering the topology of the original phylogenetic tree, as well as changing the branch lengths. We produced a collection of 50 'swapped trees', each with a 25% change in tip topology and a 25% change in node age. The function restricts each tip to moving up to two nodes from its current position. Then, for each swapped tree, we repeated all of the phylogenetic studies to confirm our results, taking into account the phylogenetic signal and calculated the total disparity. This sensitivity analysis was performed on the most comprehensive dataset including data for both the living and fossil species.

RESULTS

Relationships between variables

All linear regressions used to study relationships among continuous morphological variables of living species were found to be significant (Table 2). Phylogenetic generalized least square models returned positive and statistically significant results fitting the model to predict bone ratios from GSL. Specifically, PGLS returned significant and positive results for R/H (regression slope b = 0.065; Table 2). By contrast, the same model used to predict T/F from GSL was negative (b = −0.064; Table 2). The estimated lambda parameters for both functional ratios were close to one (Table 2). The same significant results were found using ordinary least squares regression (OLS) (Table S1). Both PGLS and OLS results were corroborated when fossil species were included in the analyses although with significant changes in the strength of the allometric effect and the parameters such as the slope (it is shallower (from 0.065 to 0.038) for the brachial index but steeper (from −0.064 to −0.103) for the crural index; Tables 2, S1).

In living mammals only, GSL showed significant associations with trophic levels and substrate preferences, while for the total sample of living *plus* fossil species, trophic levels predicted GSL as well as brachial and crural indices (Table 3). Substrate preference was associated only with GSL, while diet was a significant predictor of T/F ratio (Table 3).

Phylogenetic corrected principal component analysis

Phy–PCA returned two new vectors explaining 70.30% and 29.72% of the total variance (Fig. 1). PC1 was loaded by both R/H and T/F ratios in the same direction ($loading_{R/H} = -0.88$ and $loading_{T/F} = -0.78$). In contrast, most of the variation along PC2 was explained by changes in T/F, where the two indices contributed in opposite

TABLE 2. PGLS regression results for both living and living *plus* fossil species.

	Model	Parameter (P)		P (95% CI)	λ	λ (95% CI)
Living	R/H ~ a + b GSL	**a**	**−0.208**	**(−0.314, −0.102)**	0.933	(0.873, 0.972)
		b	**0.065**	**(0.027, 0.102)**		
	T/F ~ a + b GSL	**a**	**0.109**	**(0.029, 0.188)**	0.820	(0.702, 0.903)
		b	**−0.064**	**(−0.093, −0.034)**		
Living + fossils	R/H ~ a + b GSL	**a**	**−0.207**	**(−0.279, −0.135)**	0.939	(0.895, 0.970)
		b	**0.038**	**(0.011, 0.065)**		
	T/F ~ a + b GSL	**a**	**0.173**	**(0.110, 0.237)**	0.888	(0.805, 0.944)
		b	**−0.103**	**(−0.127, −0.078)**		

On the left of the tilde are the dependent variables (y), and on the right are the independent variables (x). The variables are: $\log_{10}$-transformed greatest skull length (GSL); $\log_{10}$-transformed radius to humerus ratio (R/H); $\log_{10}$-transformed tibia to femur ratio (T/F). Parameters (P) are the intercept (a) and the slope (b); P(95% CI) is the 95% confidence interval computed for both a and b; λ is the estimated phylogenetic signal; λ(95% CI) is the 95% confidence interval computed for λ. Parameters in **bold** are significant.

directions (R/H being positively associated ($\text{loading}_{R/H} = 0.47$) and T/F negatively ($\text{loading}_{T/F} = -0.62$)).

Mammals with a longer radius and tibia as compared to humerus and femur showed negative PC1 scores (Fig. 1). In contrast, mammals with humerus and femur longer than the radius and tibia showed positive PC1 scores (Fig. 1). PC2 values distinguished between species with longer humerus than radius and shorter femur than tibia (extremely negative values) and those with shorter humerus than radius and longer femur than tibia (extremely positive values; Fig. 1). Terrestrial mammals show a wide range of PC1 values, including extremely negative values, while other categories have values clustered on the more positive end of the distribution of scores (Fig. 1). Artiodactyla, Perissodactyla and Carnivora were widely distributed in the morphospace, while basal orders, 'Creodonta', and Cimolesta occupied the region around positive values of the first principal component (Fig. 1). Also, the ecological role categories occupied all the morphospace quadrants except non-specialized predators, which occupied the region close to the axis origin (Fig. 1). When considering the diet category, all groups were widely dispersed in the morphospace except the folivores, piscivores and omnivores (Fig. 1).

Permutation ANOVA, performed to test which ecological factors influenced the distribution of living species within the functional morphospace, showed substrate preferences and diet associated with PC2, while the habitat preference was significantly correlated with both PCs (Table 4).

We found no significant differences across substrate categories for extant species (Table 5A), while only piscivores were shown to be distinct from the other diet groups (Table 5B). For habitat, the open category differed from the closed and mixed categories along the first PC axis, whereas the wetland category differed from the open, mixed and closed categories along the second axis (Table 5C).

PGLS confirmed the permutation ANOVA results for living species (Table 6). The estimated lambdas indicated traits along the first PC more closely followed the Brownian motion relative to the second PC (Table 6).

When analysing living *plus* fossil species, both permutation ANOVA and category PGLS showed that PC1 explained differences among the substrate categories, while PC2 differences in diet (Tables 4–6). Using PGLS, we found that PC2 also differentiated the trophic level categories (Table 6). The estimated lambda was only close to 1 for PC1.

When fossil species were included in the analyses, the pairwise test, computed using the substrate category, revealed that only the amphibious and terrestrial groups were significantly different (Table 5A), although the post hoc test computed using the diet category confirmed the results obtained for the living species sample (Table 5B).

Ancestral character estimation

To include ACEs in disparity computation, the best model of evolution was fitted for both PCs extracted from the whole sample. The preferred model, based on the lowest AICc (Table 7) was lambda. Lambdas (0.94 and 0.80 for PC1 and PC2 respectively) were used to estimate ACEs and compute permutation ANOVA.

Evolutionary models were also examined to compute substrate preference for ACEs to be used in partial disparity computation (Fig. 2). Based on the lowest AICc, the best model for substrate preference was the speciational model (Table 7) with parameter kappa = 0.45.

According to the Artiodactyla substrate preferences, most of the even-toed ACEs were in the terrestrial category (Fig. 2). This was replicated for the equids lineage, while some of the ancestors of both tapirids and rhinoceros were predicted to prefer amphibious lifestyle (Fig. 2). The Cimolesta ACEs were amphibious, whereas

TABLE 3. PGLS regression results for both living and living *plus* fossil species showing the relationships between continuous and discrete variables.

	Model	*p* value	λ	λ (95% CI)
Living	GSL ~ a + b trophic level	<**0.001**	0.883	(0.773, 0.950)
	GSL ~ a + b substrate	**0.004**	0.961	(0.914, 0.989)
	GSL ~ a + b diet	0.061	0.964	(0.913, 0.994)
	R/H ~ a + b trophic level	0.096	0.937	(0.879, 0.974)
	R/H ~ a + b substrate	0.092	0.932	(0.872, 0.970)
	R/H ~ a + b diet	0.671	0.934	(0.871, 0.974)
	T/F ~ a + b trophic level	0.081	0.847	(0.738, 0.921)
	T/F ~ a + b substrate	0.060	0.879	(0.794, 0.938)
	T/F ~ a + b diet	0.093	0.861	(0.766, 0.927)
Living + fossils	GSL ~ a + b trophic level	<**0.001**	0.935	(0.887, 0.966)
	GSL ~ a + b substrate	**0.028**	0.980	(0.959, 0.994)
	GSL ~ a + b diet	0.411	0.982	(0.961, 0.996)
	R/H ~ a + b trophic level	**0.011**	0.939	(0.895, 0.969)
	R/H ~ a + b substrate	0.150	0.937	(0.891, 0.968)
	R/H ~ a + b diet	0.698	0.945	(0.901, 0.975)
	T/F ~ a + b trophic level	**0.002**	0.944	(0.890, 0.978)
	T/F ~ a + b substrate	0.076	0.964	(0.925, 0.989)
	T/F ~ a + b diet	**0.023**	0.956	(0.912, 0.985)

Results reported for living and living plus fossil species, show: *p*-value for the significance of the slope; lambda parameter estimated for the branch length transformation (λ); confidence interval for lambda estimate (95% CI). Significant values ($p<0.05$) shown in **bold**.

'Creodonta' ACEs preferred both scansorial and terrestrial habitat. Most of the Carnivora ACEs were predicted to prefer a terrestrial substrate, while the ancestors of small Caniformia and most felids were predicted to prefer a scansorial lifestyle (Fig. 2). The oldest Carnivora nodes were preferentially scansorial (Fig. 2).

Disparity analyses

Morphological disparity increased during the Paleocene (66–56 Ma) to Eocene (56–33.9 Ma) transition before declining at the end of Eocene (33.9 Ma; Fig. 3A). Total disparity remained relatively low for the entire Oligocene (33.9–23.03 Ma; Fig. 3A). About 20 Ma, the disparity curve rapidly rose reaching the maximum value during the middle Miocene (15.97–11.63 Ma; Fig. 3A). High disparity levels were maintained towards more recent times (5.333–2.58 Ma; Fig. 3A).

Partial disparity, computed to explore the diversification of different substrate preference groups, showed that terrestrial species had the greatest impact on the total disparity fluctuation, followed by the amphibious species. Other groups contributed relatively little to the total morphological disparity, particularly before the mid-Miocene (Fig. 3B).

In the earliest time periods (upper Cretaceous and Paleocene) terrestrial, scansorial and amphibious species shared comparable zeugopodia and stylopodia lengths (i.e. occupied positions close to the morphospace origin, Fig. 4).

These species were mainly represented by the ancestors of the early mammals (i.e. the ancestors of Cimolesta and Condylarthra) and by basal orders (Fig. 5). It is during the early Eocene (i.e. Ypresian stage) that terrestrial mammals with longer stylopodia as compared to zeugopodia evolved occupying the extremely positive values of PC1 (Fig. 4).

These species were represented by *Uintatherium anceps* (Dinocerata, in the basal orders group) and the cimolestan *Coryphodon molestus*. During the middle–late Eocene (i.e. Lutetian and Bartonian stages), *Juxia sharamurenensis* occupied the morphospace region of species with longer zeugopodia as compared to stylopodium (Figs 4, 5). During the entire Oligocene, the absence of species occupying the extremely positive or negative values of morphospace reflected the low morphological disparity of the entire epoch (Figs 4, 5). In the early Miocene, the extinct camelids such as *Protolabis* and merycoidodontids occupied a morphospace region partially overlapping that of modern African bovids, while the extremely positive values of PC1 were filled by large Teleoceratini and Chalicotherinii (Figs 4, 5, S3). This morphospace filling reflected the peak in morphological disparity observed during the middle Miocene (Figs 4, 5) with spatial organization remaining almost constant except for the evolution of extremely cursorial bovids and otters during the late Pliocene (Figs 4, 5).

Analyses of partial disparity showed that when disparity increased during the Eocene, the most morphologically variable group was the Perissodactyla, together with 'Creodonta', Cimolesta and basal orders (Figs 3, 5). However, the disparity of odd-toed ungulates slowly declined throughout the Oligocene. During the middle Miocene, Perissodactyla rapidly reached the highest disparity peak in their evolutionary history. We found that equids and non-equids contributed to both peaks (i.e. Eocene and middle Miocene peaks; Fig. S1). By contrast, the disparity of Artiodactyla increased slowly throughout the

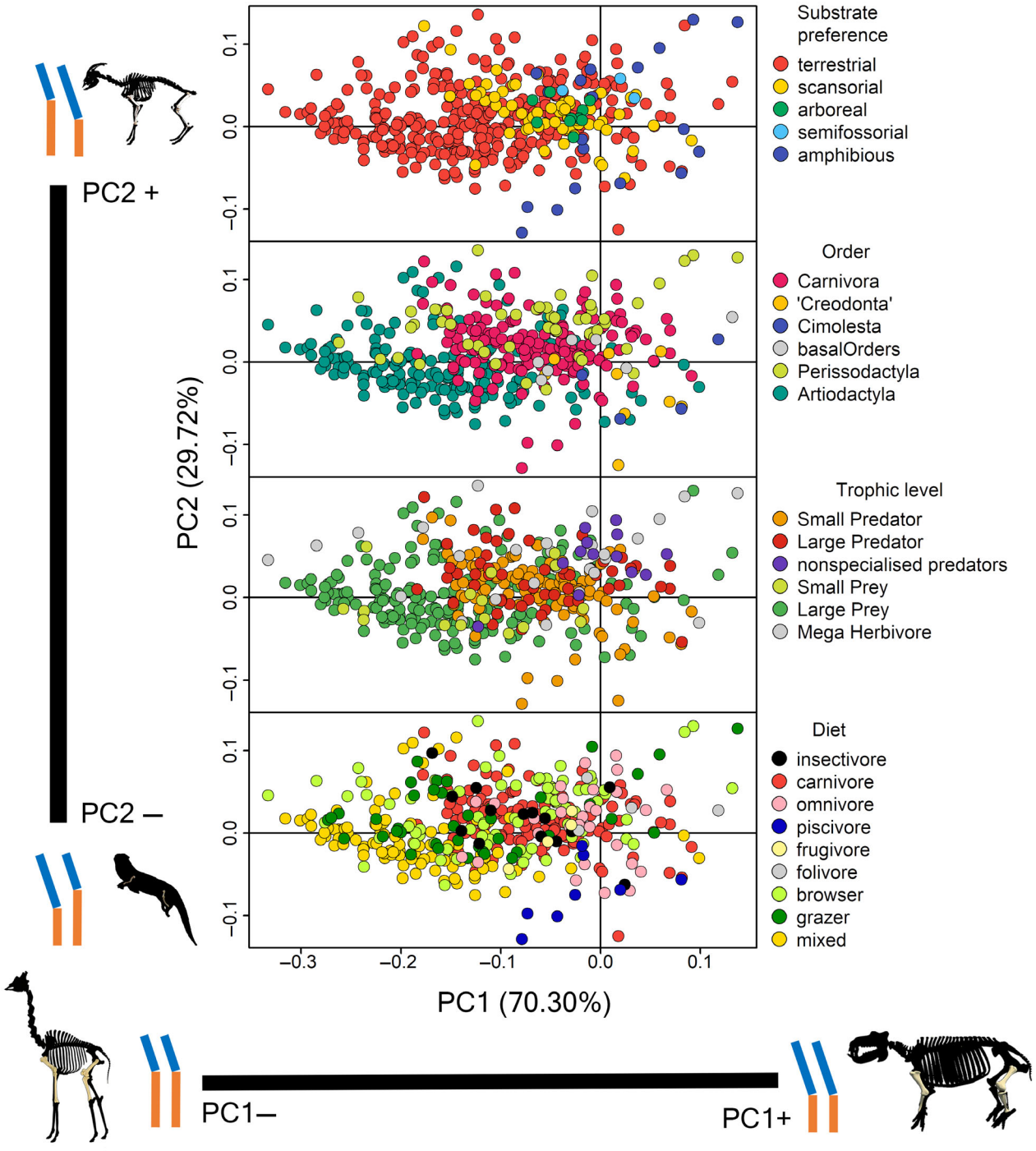

FIG. 1. Scatterplots of the first two principal component scores. Dots are coloured according to substrate preference, order, trophic level, and diet categories. *Giraffa camelopardalis* shows negative PC1 values, *Hippopotamus amphibius* shows positive PC1 values. *Capra* shows positive PC2 values and *Pteronura brasiliensis* shows negative PC2 values. PC plots were generated in R.

Cenozoic and peaked at *c.* 15 Ma in the middle Miocene (Fig. 3). Carnivores mirrored the even-toed ungulates and they had a minor contribution to the overall disparity with a small diversification event occurring by the end of the Oligocene (Fig. 3C, F). They only contributed significantly to total disparity during the last *c.* 15 Ma.

The inclusion of the ACEs to calculate disparity over time did not change the overall trend observed with tip

TABLE 4. Permutation ANOVA *p*-values.

Taxa	Trait	Trophic level	Substrate	Diet	Habitat
Living species	PC1	0.696	0.116	0.608	**0.012**
	PC2	0.430	**0.009**	**0.006**	$\mathbf{9.99 \times 10^{-5}}$
Living + fossil species	PC1	0.573	**0.041**	0.323	–
	PC2	0.087	0.084	**0.011**	–

Significant values ($p<0.05$) shown in **bold**.

species only (Fig. 3A, D). The larger temporal window showed a very low disparity during the late Cretaceous (Fig. 3D–F).

Effect of temperature and primary productivity

PCA, performed to summarize the mean, median and variance of the stable isotopes $\delta^{18}O$ and $\delta^{13}C$ fluctuations, returned six axes. PC1 and PC2 explained 92% and 8% of the total variance, respectively. Oxygen fluctuation strongly influenced change along PC1 ($loading_{mean\delta18O} = 0.652$; $loading_{median\delta18O} = 0.650$). Carbon was loaded negatively on the same axis ($loading_{mean\delta13C} = -0.275$; $loading_{median\delta13C} = -0.276$). By contrast, PC2 mainly represented carbon fluctuation ($loading_{mean\delta13C} = 0.641$, $loading_{median\delta13C} = 0.661$). Lower PC1 values described stages with extremely high temperatures and low primary productivity such as Paleocene and Eocene. The opposite values were associated with extremely cold stages with high primary productivity (Fig. 6).

SDE results suggested that there was no connection between climatic changes and mammalian disparity with (tips plus nodes case) and without (tips case) accounting for the incompleteness of the fossil species (Table 8). In all cases, the highest maximum likelihood and posterior probability was returned for model 1 supporting no connection between climate and mammalian disparity.

In both tips and tips + nodes cases, the highest likelihood and percentage of posterior probability supported model 4 for the relationships between Carnivora and Artiodactyla disparity assuming that the disparities of both orders were two-way favourably strongly connected (Table 9). Model 3, assuming a casual connection, was the favourite model describing the relationships between Perissodactyla, with both Artiodactyla and Carnivora disparities (Table 9). Equally, the highest likelihood and posterior probability were returned for model 3 in the relationships between 'Creodonta' disparity which was found to be casually linked to Carnivora disparity (Table 9).

Artiodactyla and Carnivora were probably casually linked with a bi-directional model; in the tips case β Artiodactyla to Carnivora is 0.067 (−1.055, 0.904; Table 10) suggesting that a high disparity of Artiodactyla were related to the high disparity of Carnivora and *vice versa*. These results were supported also when node values were included in the analyses (Table 10). β Carnivora to Artiodactyla was higher than β Artiodactyla to Carnivora in both tips (0.550) and tips *plus* nodes (0.485) cases, suggesting the effect of Carnivora was the strongest. The parameters estimated for the relationships between Perissodactyla and both Artiodactyla and Carnivora returned positive and negative β values, respectively. The β values suggested that high disparity values in the odd-toed clade were linked to low disparity levels in Carnivora and high in Artiodactyla (Table 10). The same pattern linking Perissodactyla to Carnivora was observed Carnivora and 'Creodonta' with the latter group being negatively influenced by Carnivora (Table 10).

Phylogenetic uncertainty

On average, the set of 'swapped trees' was 65.14% comparable to the original tree (CI: 64.05–68.36%), and the phylogenetic analyses calculated using these trees mirrored the results of the original analyses. PGLS regressions computed to evaluate the relationship between collected variables (i.e. R/H ~ GSL and T/F ~ GSL) were significant in 100% of random trees. Both PC1 and PC2, which were created from 50 Phy–PCA based on swapped trees, were found to evolve according to lambda in 100% cases. Regarding the permutation ANOVA, we found significant variation in substrate preferences along the PC1 60% of the time, but only 34% of the time along the PC2. As regards to the trophic level category, ANOVA results resembled the real one 100% of cases for PC1 and 60% of cases for PC2, while the PGLS 100% for PC1 and 68% for PC2. Category PGLS supported 100% of the real results for the diet category. Finally, the disparity results also resembled the real disparity computed for tips 100% of cases (Serio *et al.* 2024, data 6).

DISCUSSION

In this work, we investigated the morphological disparity of the two long bones functional ratios, the brachial and crural indices, throughout the Cenozoic. Our findings revealed that variations in stable isotopes $\delta^{18}O$ and $\delta^{13}C$, which were used as proxies for palaeotemperature and primary productivity, did not affect morphological diversification of ecological groups or clades. On the other hand, it was shown that clade interaction and/or

TABLE 5. TukeyHSD post-hoc computed on substrate preference (A), diet (B), and habitat (C).

A Substrate

	Living		Living + fossil	
	TukeyHSD PC2		TukeyHSD PC1	
	Z	*p* value	Z	*p* value
Amphibious–arboreal	−0.339	0.632	−1.149	0.860
Amphibious–scansorial	1.400	0.079	0.627	0.285
Amphibious–semifossorial	1.497	0.067	−0.872	0.795
Amphibious–terrestrial	1.183	0.121	1.646	**0.044**
Arboreal–scansorial	0.700	0.253	0.560	0.309
Arboreal–semifossorial	1.194	0.116	−1.335	0.899
Arboreal–terrestrial	0.353	0.382	1.334	0.091
Scansorial–semifossorial	0.657	0.261	0.165	0.447
Scansorial–terrestrial	0.108	0.476	1.033	0.160
Semifossorial–terrestrial	0.929	0.176	0.674	0.264

B Diet

Pairs	Living		Living + fossil	
	TukeyHSD PC2		TukeyHSD PC2	
	Z	*p* value	Z	*p* value
Browser–carnivore	−0.095	0.547	0.555	0.307
Browser–folivore	−0.229	0.596	0.129	0.458
Browser–frugivore	−0.498	0.699	−0.183	0.579
Browser–grazer	−0.514	0.692	−0.745	0.766
Browser–insectivore	−0.558	0.706	−0.692	0.748
Browser–mixed	0.893	0.195	1.166	0.128
Browser–omnivore	−0.650	0.735	1.141	0.131
Browser–piscivore	3.082	**<0.001**	2.700	**0.001**
Carnivore–folivore	0.251	0.412	0.550	0.304
Carnivore–frugivore	−0.962	0.835	−0.862	0.795
Carnivore–grazer	0.611	0.296	0.708	0.260
Carnivore–insectivore	−2.051	0.981	−1.098	0.849
Carnivore–mixed	0.542	0.319	−0.006	0.519
Carnivore–omnivore	−1.313	0.891	0.379	0.376
Carnivore–piscivore	3.020	**<0.001**	2.487	**0.003**
Folivore–frugivore	−0.088	0.545	0.381	0.372
Folivore–grazer	−0.690	0.752	−0.106	0.553
Folivore–insectivore	0.090	0.476	0.257	0.410
Folivore–mixed	0.623	0.273	0.750	0.237
Folivore–omnivore	0.072	0.486	0.896	0.195
Folivore–piscivore	2.616	**0.002**	2.141	**0.012**
Frugivore–grazer	−0.205	0.587	−0.004	0.510
Frugivore–insectivore	−0.959	0.835	−0.706	0.753
Frugivore–mixed	−2.889	0.998	−1.599	0.939
Frugivore–omnivore	−0.831	0.802	−1.416	0.912
Frugivore–piscivore	1.412	0.072	1.282	0.096
Grazer–insectivore	0.106	0.476	−0.278	0.613
Grazer–mixed	1.376	0.084	1.180	0.124
Grazer–omnivore	0.097	0.477	1.218	0.115
Grazer–piscivore	3.205	**<0.001**	2.690	**0.001**
Insectivore–mixed	−0.172	0.571	−0.297	0.622
Insectivore–omnivore	−1.608	0.936	0.103	0.475
Insectivore–piscivore	2.840	**0.001**	2.179	**0.009**
Mixed–omnivore	0.180	0.447	−0.407	0.657
Mixed–piscivore	2.866	**0.001**	2.290	**0.006**
Omnivore–piscivore	2.949	**0.001**	1.971	**0.018**

C Habitat

Pairs	Living			
	TukeyHSD PC1		TukeyHSD PC2	
	Z	*p* value	Z	*p* value
Closed–mixed	0.908	0.198	−2.169	0.988
Closed–open	2.952	**0.000**	1.195	0.118
Closed–wetland	−0.081	0.540	2.876	**0.001**
Mixed–open	2.326	**0.005**	1.425	0.073
Mixed–wetland	−1.105	0.850	2.924	**0.001**
Open–wetland	−0.016	0.518	3.196	**0.000**

Results were reported for living (A, B, C) and living + fossil species (A, B). Significant values ($p<0.05$) shown in **bold**.

competition were likely to have impacted changes in the morphological disparity of mammals.

Even though the relationships were not particularly strong, we discovered that both the radius/humerus and the tibia/femur ratios were significantly associated with the greatest skull length. These regressions produced different slope values when living and living *plus* fossil species were considered (Table 2), indicating that fossils are a significant addition to this type of study. Christiansen's (2002) study, for example, proposes a universal equation to determine the long bone ratio, which does not appear to be valid when including fossil taxa. Many extinct species had morphologies with no extant equivalent, especially in the proportion of the hind limbs, where we noted greater changes in slope and intercept parameters.

The functional morphospace (Fig. 1) was informative mainly about substrate preference and may help our understanding of limb bone evolution. Mammals with shorter legs were opposed to extant cursorial ungulates such as giraffids, camelids, pecorans, ruminants and equids. The cursorial ungulates share the same region with canids and most pantherines which, even though

TABLE 6. Category PGLS results.

	Model	*p* value	λ	95% CI
Living species	Trophic level ~ a + b PC1	0.706	0.924	(0.863, 0.965)
	Trophic level ~ a + b PC2	0.475	0.715	(0.522, 0.852)
	Substrate ~ a + b PC1	0.120	0.919	(0.856, 0.961)
	Substrate ~ a + b PC2	**0.005**	0.763	(0.616, 0.870)
	Diet ~ a + b PC1	0.639	0.921	(0.856, 0.964)
	Diet ~ a + b PC2	**0.003**	0.702	(0.529, 0.834)
	Habitat ~ a + b PC1	**0.011**	0.911	(0.842, 0.958)
	Habitat ~ a + b PC2	<**0.001**	0.717	(0.555, 0.839)
Living + fossil species	Trophic level ~ a + b PC1	0.508	0.947	(0.905, 0.975)
	Trophic level ~ a + b PC2	0.058	0.762	(0.622, 0.862)
	Substrate ~ a + b PC1	0.317	0.950	(0.907, 0.979)
	Substrate ~ a + b PC2	0.001	0.749	(0.607, 0.852)
	Diet ~ a + b PC1	0.306	0.951	(0.908, 0.979)
	Diet ~ a + b PC2	**0.001**	0.751	(0.610, 0.853)

Results reported for living and living + fossil species groups show: *p*-value for the significance of the slope; lambda parameter estimated for the branch length transformation (λ); confidence interval for lambda estimate (95% CI); the fraction of variance of the dependent variable explained by the independent variable (R2). Significant values ($p<0.05$) shown in **bold**.

they occupy positions close to zero (i.e. the origin of the axes), overlap with ungulate morphospace, suggesting convergence in the evolution of cursorial adaptation between large predators and prey (Figs S2–S5). Ungulates evolved extreme 'cursorial adaptations' such as fused radius and ulna, and the reduced fibula (Janis & Wilhelm 1993; Polly 2007), and shared the longer radii and tibia relative to the humerii and femora found in carnivores.

The differences in bone proportions, which defined the distribution of species into the functional morphospace, are not explained by phylogeny alone. Ungulates, which are more variable than Carnivora, include different morphotypes ranging from the terrestrial equids, bovids and cervids to the robust amphibious hippopotamus and *Teleoceras*. Amphibious, arboreal and semi-fossorial species are found in the same morphospace region while terrestrial and scansorial species are more widely dispersed (Fig. 1).

The morphological disparity of long bone ratios was found to be especially high in two epochs: the Eocene and Miocene. This pattern was not mirrored by sample size, which increased throughout the Paleocene and Pleistocene, or species diversity calculated using data from the PBDB. In the case of species diversity, the larger increase in diversity during the Miocene happened slightly earlier than the morphological disparity (Fig. S6).

Our analysis of morphological disparity suggests that major diversification events in carnivores and ungulate limb bones were probably due to clade interaction and were independent of environmental conditions. During the late Cretaceous, mammalian disparity was low amongst the ancestors of Cenozoic mammals, which were mainly arboreal, occupying the region of the morphospace close to the axis origin (Fig. 3). However, the K–Pg extinction caused a reduction in arboreal habitat and terrestrial species were able to diversify, occupying vacated niches. The analysis of morphological tarsal disparity in early mammals returned similar results, suggesting terrestriality was the key innovation to support diversification in early mammals during the Paleocene–Eocene interval (66–33 Ma; Shelley *et al.* 2021). In addition, as Carnivora shared a plesiomorphic scansorial habit (Flynn *et al.* 2010) our results showed that it was mainly ungulates such as the perissodactyls *Hyracotherium*, *Hyrachyus* and

TABLE 7. Values of the Akaike information criterion corrected for sample size (AICc) for the different evolutionary models for the five different analyses of continuous and discrete data.

Taxa	Trait	BrM	OU	EB	Lambda	Kappa	Delta
Living species	PC1	−800.657	−808.617	−798.607	**−824.839**	−815.107	−807.083
	PC2	−975.613	−1006.409	−973.563	**−1021.340**	−987.488	−995.130
Living + fossil species	PC1	−1265.775	−1275.379	−1263.746	**−1288.101**	−1287.412	−1264.112
	PC2	−1587.884	−1639.432	−1585.854	**−1651.249**	−1619.827	−1594.910
	Substrate	409.612	–	410.112	407.197	**402.578**	411.160

The models are: Brownian motion (BrM); Ornstein–Uhlenbeck (OU); early burst (EB); lambda, kappa, delta. The best models are shown in **bold**.

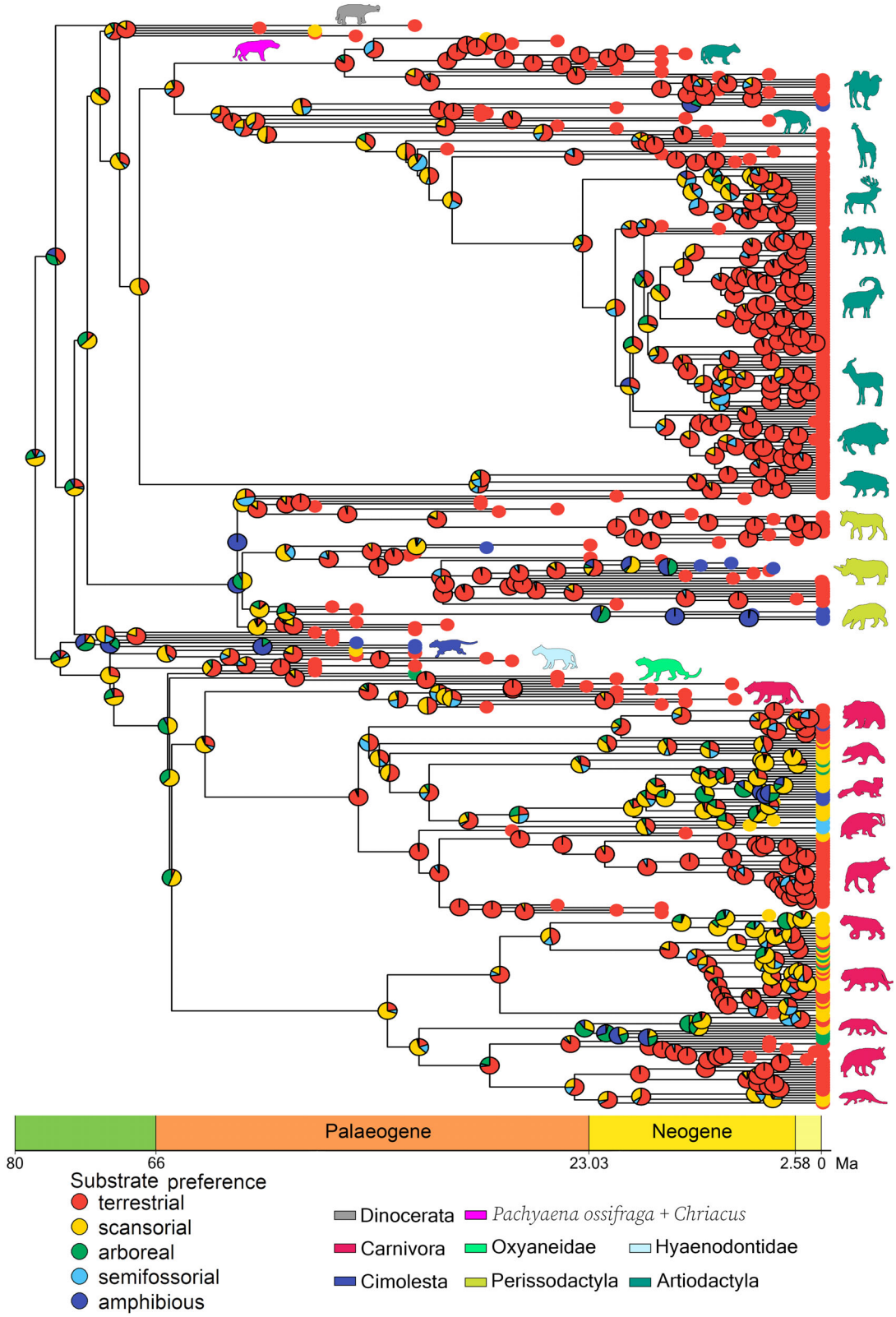

FIG. 2. Phylogenetic tree of 420 mammalian species. Tip dots are coloured according to the substrate. Pie charts are coloured according to the substrate posterior probabilities of ACE estimated for each node. (Silhouettes from https://www.phylopic.org/; copyright information provided in Appendix S2.)

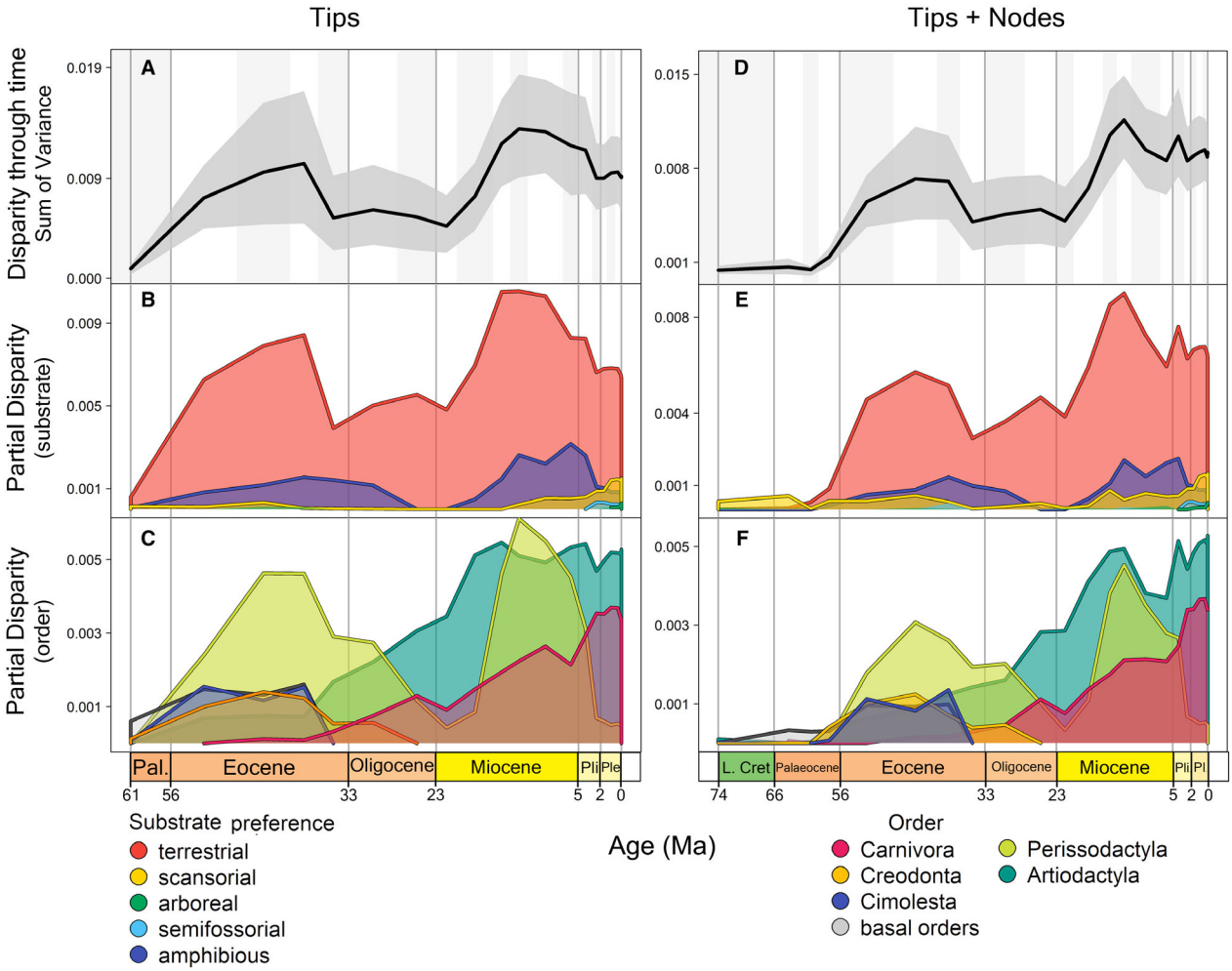

FIG. 3. A, morphological disparity through time computed for carnivores and ungulates throughout the Cenozoic in 22 time period bins based on the sum of variance metric (from 2 PC axes and rarefied to the median sample size for all 22 bins, n = 31). B, partial disparity computed according to the substrate categories. C, partial disparity computed for orders. D, disparity through time (computed taking into account ACEs) throughout the Cenozoic; 25 bins based on the sum of variance metric (from 2 PC axes and rarefied to the median sample size for all 21 bins, n = 49). E, partial disparity computed for the substrate categories and taking into account the ACE values. F, partial disparity computed for orders and taking into account the ACE values. Grey areas in A and D represent confidence intervals which were obtained from the 500 bootstrap replicates.

Parvicornus, both the basal orders Dinocerata and Condylarthra, and 'Creodonta', with longer zeugopodia compared to stylopodia, that contributed to the first adaptive radiation of terrestrial species. This idea is supported by the high disparity values of the Perissodactyla, 'Creodonta', and basal orders during the Palaeogene (Figs 3–5).

During the Eocene, many Carnivora families such as Canidae, Mustelidae, Ursidae, Amphicyonidae and Nimravidae originated all at once (Flynn *et al.* 2010). Hence, we supposed the emergence of new taxa resulted in the second adaptive radiation among terrestrial and amphibious species. At this time, we found also amphibious species were represented by *Coryphodon*, Pantolestidae, and *Metamynodon* sharing longer humerii and femurs as opposed to short radii and tibiae.

During the Eocene–Oligocene interval (56–23 Ma) long-legged ungulates evolved in North America (Garland & Janis 1993; Janis & Wilhelm 1993; Levering *et al.* 2017). Our results showed that by the end of the Oligocene, species such as *Michenia* or *Miohippus* demonstrated the first cursorial features, such as longer radius and tibia, and occupied the morphospace region of living camelids and horses. During the Miocene (23–5 Ma), we found that the morphospace of living cursorial ruminants and cervids became filled by their ancestors and long-legged carnivores, such as the ancestors of the living canids, evolved. These findings support those of Janis & Wilhelm (1993)

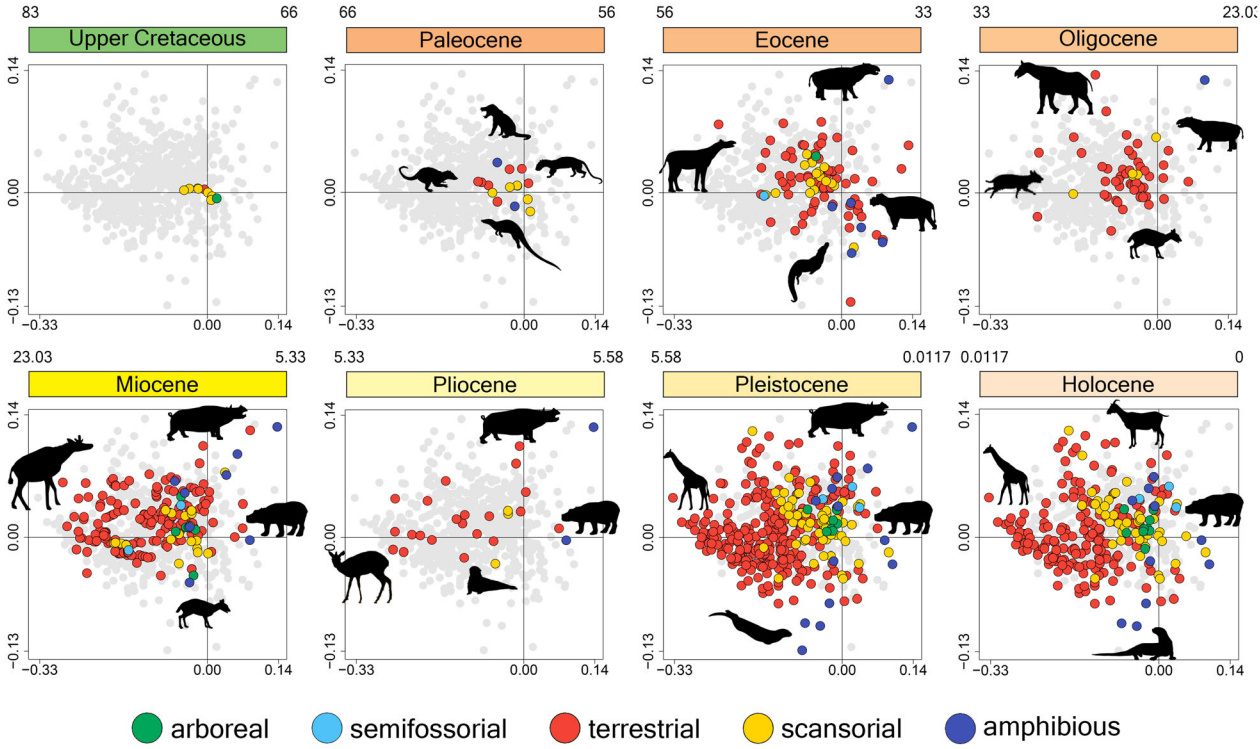

FIG. 4. Morphospace occupation of the substrate preference category throughout the Cenozoic. Stages were collapsed according to the Epoch to which they belong. Grey points represent the entire database. (Silhouettes from https://www.phylopic.org/; see Appendix S2 for copyright information.)

and Flynn *et al.* (2010). All of these changes are reflected in the scansorial disparity peak we found at about 15 Ma. It is noteworthy that early Miocene scansorial carnivores occupied morphospace regions similar to those of Recent ones. The same observation was made by Goswami & Friscia (2010) who suggested that the Carnivora diversified early in their locomotor preferences and remained almost constant throughout the Cenozoic. This pattern is supported by similar findings for the feeding apparatus. Wesley-Hunt (2005), Meloro & Raia (2010), and Meloro (2011b) suggested that this evolutionary stasis resulted from resource partitioning to reduce competition, occupying different locomotor and feeding habits in living carnivores. Studies of the well-preserved fossil record suggest the same partitioning in the past. Considering that the history of carnivores was characterized by iterative evolution, our results showed that the morphospace occupation remained constant for long bones because of the repeated evolution of specific morphologies at different points in time (Van Valkenburgh 2007). The iterative evolution of similar ecomorphologies suggests that other factors besides changes in limb morphology, such as reproductive physiology, may have driven evolution at this stage (Clauss *et al.* 2019).

We found that morphospace occupation has remained almost unchanged since the Pliocene. The partial disparity analysis revealed a significant turnover between 'Creodonta' and Carnivora during the Palaeogene, supporting a double-wedge model (Benton 1987; Van Valkenburgh 1999). 'Creodonta' were the Eocene's dominant predators. Compared to Carnivora predators, most 'Creodonta' showed morphotypes with stylopodia longer than zeugopodia and filled a small morphospace region (Fig. 5). 'Creodonta' had a significant degree of morphological differentiation up to the middle of the Eocene, at which point Carnivora's disparity began to rise, reaching the first peak during the middle of the Oligocene. Our findings indicate that Carnivora disparity probably had a negative impact on 'Creodonta' disparity, supporting the findings of Flynn *et al.* (1998) and Van Valkenburgh (1999) that pointed towards clade competition as the reason for the turnover between these two predatory groups. 'Creodonta' were large body-size species that reached sizes never reached by Carnivora, and Janis & Wilhelm (1993) demonstrated that Hyaenodonta had a hunting style that was different from modern predators and probably less effective in prey capture. A double-wedge pattern has already been proven to occur among other clades such as the Hathliacynidae (Sparassodonta) and some Didelphoidea (Zimicz 2014), as well as brachiopods and bivalves (Sepkoski 1996).

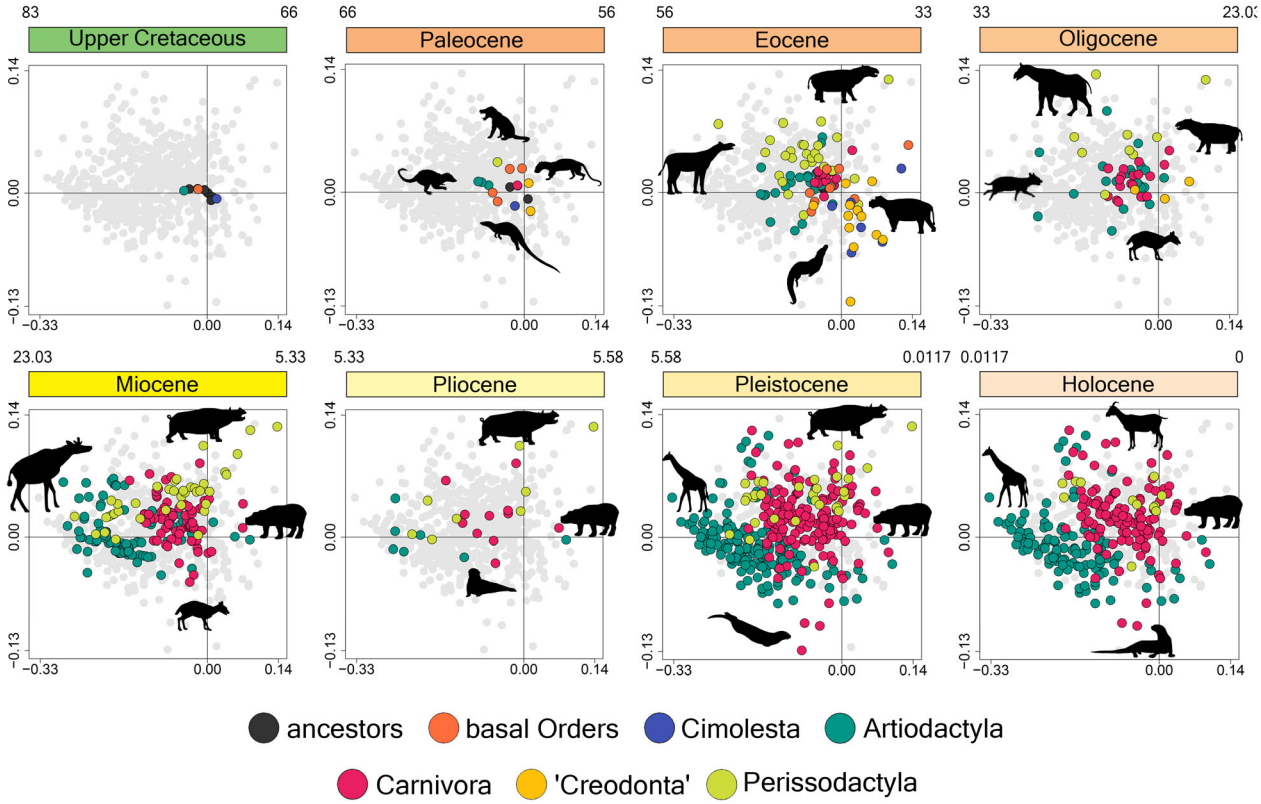

FIG. 5. Morphospace occupation of the orders throughout the Cenozoic. Stages were collapsed according to the Epoch to which they belong. Grey points represent the entire database. (Silhouettes from https://www.phylopic.org/; see Appendix S2 for copyright information.)

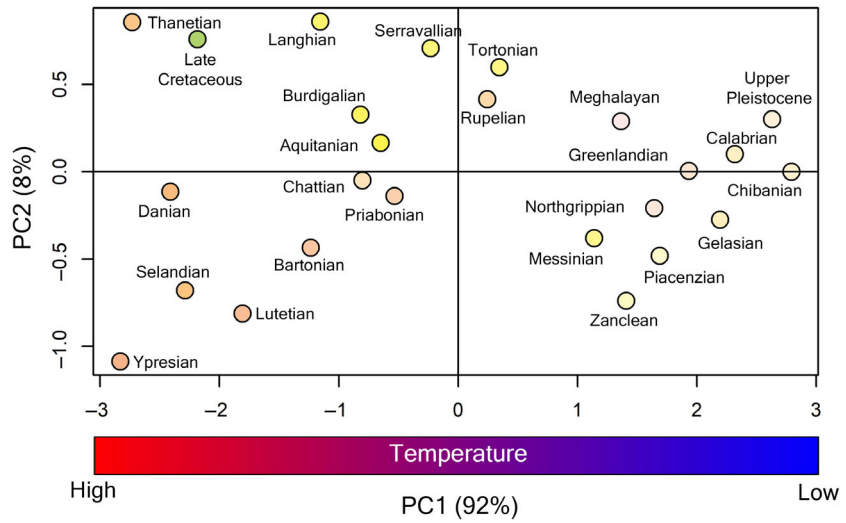

FIG. 6. Scatterplot of PC axis returned for climatic variables.

The partial disparity analysis throughout the Cenozoic showed Perissodactyla had a greater morphological disparity than Artiodactyla during the Eocene. The extinction of amphibious morphotypes during the Oligocene indicates a decline in Perissodactyla disparity, but the emergence of early camelids, hypertragulids and

TABLE 8. Causal connection between climate and mammalian disparity; maximum likelihood and Bayesian posterior probabilities for different models.

Cause	Effect	Tips				Tips + nodes			
		Model 1		Model 2		Model 1		Model 2	
		ML	PP (%)	ML	PP (%)	ML	PP (%)	ML	PP (%)
Climate	Total disparity	**63.092**	**82.437**	61.546	17.563	**71.162**	**88.966**	69.075	11.034
Climate	Terrestrial	**66.542**	**86.576**	64.678	13.424	**76.032**	**91.748**	73.624	8.252
Climate	Scansorial	**95.702**	**91.674**	93.304	8.327	**103.330**	**98.739**	98.969	1.261
Climate	Arboreal	**116.669**	**99.999**	104.993	0.001	**131.976**	**100.000**	118.277	0.000
Climate	Semifossorial	**112.089**	**95.868**	108.945	4.132	**125.296**	**99.996**	115.130	0.004
Climate	Amphibious	**81.102**	**98.043**	77.188	1.957	**94.663**	**98.575**	90.426	1.425
Climate	Carnivora	**87.011**	**88.488**	84.972	11.512	**97.175**	**83.042**	95.586	16.958
Climate	Artiodactyla	**83.048**	**82.087**	81.526	17.913	**88.536**	**90.214**	86.315	9.786
Climate	Perissodactyla	**69.386**	**90.990**	67.074	9.010	**82.016**	**95.833**	78.881	4.167
Climate	'Creodonta'	**98.130**	**96.526**	94.805	3.474	**111.546**	**98.098**	107.603	1.902
Climate	Basal orders	**92.224**	**98.490**	88.046	1.510	**109.430**	**98.941**	104.892	1.059

ML, maximum likelihood; PP, Bayesian posterior probability. Model 1: no connections between climate and disparities; Model 2: causal connection from climate to disparities. The best models are shown in **bold**.

TABLE 9. The causal connection among mammalian disparities; maximum likelihood and Bayesian posterior probabilities for different models.

Cause	Effect	Tips									
		Model 1		Model 2		Model 3		Model 4		Model 5	
		ML	PP (%)	ML	PP (%)	ML	PP (%)	ML	PP (%)	ML	PP (%)
Car	Art	217.675	16.512	218.208	28.149	217.915	21.008	**218.407**	**34.331**	85.159	0.000
Car	Per	204.009	19.851	204.016	19.987	**204.295**	**26.412**	204.216	24.420	203.254	9.330
Art	Per	200.018	23.377	199.851	19.775	**200.118**	**25.824**	199.951	21.871	199.081	9.154
Car	Cre	232.727	24.187	232.604	21.388	**232.728**	**24.222**	232.581	20.910	231.770	9.292
Cause	Effect	Tips + nodes									
		Model 1		Model 2		Model 3		Model 4		Model 5	
		ML	PP (%)	ML	PP (%)	ML	PP (%)	ML	PP (%)	ML	PP (%)
Car	Art	252.988	8.208	253.837	19.181	253.883	20.094	**254.201**	**27.625**	254.097	24.892
Car	Per	246.546	19.348	246.407	16.833	**246.943**	**28.783**	246.720	23.038	246.068	11.998
Art	Per	237.850	28.001	237.647	22.867	**237.910**	**29.746**	82.284	0.000	237.482	19.386
Car	Cre	276.043	29.297	275.689	20.576	**276.043**	**29.319**	275.700	20.808	90.181	0.000

Art, Artiodactyla; Car, Carnivora; Cre, 'Creodonta'; ML, maximum likelihood; Per, Perissodactyla; PP, Bayesian posterior probability. Model 1: No connections between the morphological disparity of two competing orders; Model 2: Causal connection from Order 1 disparity to Order 2 disparity; Model 3: Causal connection from Order 2 disparity to Order 1 disparity; Model 4: Causal connections from Order 1 disparity to Order 2 disparity and from Order 2 disparity to Order 1 disparity (2-way feedback system); Model 5: Correlative connection between Order 1 disparity and Order 2 disparity. The best models are shown in **bold**.

merycoidodonts reflects a rise in Artiodactyla disparity. Our results showed that during the Miocene, Perissodactyla disparity rebounded and Artiodactyla disparity peaked. However, Artiodactyla disparity remained nearly constant after the Miocene while Perissodactyla disparity declined significantly. Perissodactyla was broadly spread in the morphospace, with both terrestrial and amphibious morphotypes, whereas Artiodactyla was restricted to primitive morphotypes (Fig. 5).

Even if our SDE findings indicated that Artiodactyla disparity positively influenced the Perissodactyla disparity, the β value, indicating the strength of the causal

TABLE 10. Parameter estimates from the best models.

Relationship between Artiodactyla & Carnivora disparity model 4

	Tips				Tips + nodes			
	Mean	Median	Lower bound (95%)	Upper bound (95%)	Mean	Median	Lower bound (95%)	Upper bound (95%)
α Artiodactyla	1264.317	64.830	5.932	9628.882	626.903	76.457	3.826	4248.293
μ Artiodactyla	0.002	0.002	−0.018	0.028	0.003	0.003	−0.008	0.015
σ Artiodactyla	0.000	0.000	0.000	0.001	0.000	0.000	0.000	0.001
α Carnivora	1549.807	156.572	4.948	11 922.130	460.467	70.873	2.791	2957.692
μ Carnivora	0.003	0.001	−0.013	0.033	0.002	0.002	−0.005	0.009
σ Carnivora	2.95×10^{-4}	2.85×10^{-4}	1.87×10^{-4}	4.64×10^{-4}	2.73×10^{-4}	2.59×10^{-4}	1.68×10^{-4}	4.75×10^{-4}
β Artiodactyla to Carnivora	0.067	0.145	−1.055	0.904	0.145	0.284	−0.912	0.814
β Carnivora to Artiodactyla	0.550	0.583	−0.745	1.627	0.485	0.485	−0.717	1.464

Relationship between Perissodactyla & Carnivora disparity model 3

	Tips				Tips + nodes			
α Perissodactyla	670.787	27.538	3.364	4032.547	425.963	28.121	4.147	2146.304
μ Perissodactyla	0.004	0.002	−0.011	0.044	0.000	0.001	−0.018	0.006
σ Perissodactyla	0.001	0.001	0.001	0.002	0.001	0.001	0.000	0.001
α Carnivora	1849.291	138.017	16.877	14 677.140	1031.000	129.218	18.816	7649.220
μ Carnivora	0.003	0.002	−0.012	0.028	0.001	0.001	−0.020	0.011
σ Carnivora	0.000	0.000	0.000	0.000	2.51×10^{-4}	2.48×10^{-4}	1.47×10^{-4}	3.68×10^{-4}
β Perissodactyla to Carnivora	−0.138	−0.187	−1.098	0.915	−0.145	−0.149	−1.110	1.003

Relationship between Perissodactyla & Artiodactyla disparity model 3

	Tips				Tips + nodes			
α Perissodactyla	412.783	18.887	2.700	2893.361	258.766	19.064	3.840	2254.768
μ Perissodactyla	0.003	0.002	−0.011	0.022	0.002	0.001	−0.008	0.018
σ Perissodactyla	0.001	0.001	0.001	0.002	0.001	0.001	0.000	0.001
α Artiodactyla	3871.074	179.635	22.893	12 125.700	1959.769	180.984	22.824	8943.113
μ Artiodactyla	0.002	0.003	−0.018	0.023	0.002	0.002	−0.016	0.020
σ Artiodactyla	0.000	0.000	0.000	0.001	3.9×10^{-4}	3.8×10^{-4}	2.3×10^{-4}	5.9×10^{-4}
β Perissodactyla to Artiodactyla	0.052	0.068	−1.021	1.058	0.037	0.030	−0.977	1.060

Relationship between 'Creodonta' & Carnivora disparity model 3

	Tips				Tips + nodes			
α 'Creodonta'	360.429	62.592	10.243	2440.358	746.790	56.809	10.508	4650.180
μ 'Creodonta'	3×10^{-4}	2.9×10^{-4}	−0.003	0.003	0.000	2×10^{-4}	−0.003	0.003
σ 'Creodonta'	1.5×10^{-4}	1.5×10^{-4}	1.1×10^{-4}	2.2×10^{-4}	1.3×10^{-4}	1.2×10^{-4}	9.2×10^{-5}	1.8×10^{-4}
α Carnivora	1801.261	143.812	15.541	14 008.070	2886.285	202.828	17.701	18 210.280
μ Carnivora	0.002	0.002	−0.012	0.017	0.001	0.001	−0.014	0.016
σ Carnivora	3×10^{-4}	2.9×10^{-4}	1.9×10^{-4}	4.5×10^{-4}	2.6×10^{-4}	2.6×10^{-4}	1.7×10^{-4}	3.8×10^{-4}
β 'Creodonta' to Carnivora	−0.048	−0.055	−1.039	1.009	−0.038	−0.040	−1.008	0.942

α: strength; μ: mean value; σ: standard deviation; β: strengths of the Granger causal link between two time series. Estimated values are presented for the mean, median and lower and upper bounds of the best models shown in Table 9.

connection, is close to zero suggesting that other factors may have played a major role in the decline of Perissodactyla disparity. By the end of the Oligocene, Perissodactyla disparity rapidly declined while Artiodactyla disparity increased (Fig. 3). The turnover between Perissodactyla and Artiodactyla has already been reported, with morphological changes in teeth, limbs and digestive systems, including the use of the gastrointestinal microbes not only as symbiotic digestive service providers but as farmed prey, potentially providing advantages for Ruminantia in competition for similar niches (Benton 1983; Clauss *et al.* 2023), but differing reproductive physiology may also have played a role (Clauss *et al.* 2019). Janis (1989) argued that this trend was primarily driven by climate and vegetation change, although our findings support the hypotheses of Benton (1983) and Clauss *et al.* (2019). However, in this scenario, we need to keep in mind that our environmental proxies do not include plant type, which changed throughout the Cenozoic and was most likely the principal cause of ungulate morphological diversity. In terms of tooth shape, feeding strategy, and cursorial adaption, the more specialized artiodactyls may have superseded the less specialized perissodactyls until equid diversification occurred during the middle Miocene (Janis 1989; Cantalapiedra *et al.* 2017). To corroborate this theory, Levering *et al.* (2017) demonstrated that among North American ungulates, Artiodactyla developed towards a more cursorial morphotype, improving locomotory capabilities, while Perissodactyla limb length remained constant throughout the Cenozoic.

Our findings also revealed that Perissodactyla disparity negatively influenced Carnivora disparity. We suggest that the odd-toed clade had a negative impact on the predator clade since the majority of Perissodactyla were megaherbivores, whereas Carnivora variability was possibly mainly influenced by equid diversity. Interestingly β appears not to be extremely high suggesting that more factors could be at play to explain the observed pattern.

Another interesting outcome of our disparity analysis was the support for a positive effect of Artiodactyla disparity on Carnivora disparity and *vice versa*. Figure 3 indicates that both orders followed the same patterns throughout the Cenozoic, even though the Artiodactyla disparity always remained relatively higher. This suggests a link between the clades including the mainly large predators and their prey. However, caution is required to interpret this pattern in the light of predator–prey interaction because the Carnivora also includes non-specialized predators while the Artiodactyla includes several taxa immune to predation such as the amphibious hippopotamus. The two clades might have simultaneously benefited from the extinction of short-legged morphologies in their more closely related competitors such as creodonts and perissodactyls, leading to peaks in morphological diversity during periods of open habitat spreading (Middle Miocene and Pliocene).

CONCLUSION

We have tested the effects of four different ecological categories on the evolution of long bones in a large sample of terrestrial mammals. Substrate preference was the best predictor of occupation of functional morphospace and distinguished between stocky amphibious and terrestrial mammals. Terrestrial mammals appear to be the principal responsible of increased disparity during the Cenozoic, while clade interaction and competition were found to be the main drivers for temporal fluctuations in morphological disparity.

Acknowledgements. We are grateful to Peter Falkingham, Claudia Mettke-Hoffman, Rui Martiniano (LJMU) for commenting on early versions of this manuscript. Nicolas Navarro also supported to solve issues in partial disparity calculations. We also want to thank the Editor Dr Mary Silcox, Dr Sally Thomas, and two anonymous referees for their feedback, which helped us improve the manuscript.

Author contributions. **Conceptualization** C Serio (CS), RP Brown (RPB), M Clauss (MC), C Meloro (CM); **Data Curation** CS, CM; **Formal Analysis** CS, CM; **Investigation** CS, CM; **Methodology** CS, CM, RPB, MC; **Software** CS; **Supervision** CM, RPB, MC; **Validation** CM, RPB, MC; **Visualization** CS; **Writing – Original Draft** CS; **Preparation** CS; **Writing – Review & Editing** CS, CM, RPB, MC.

DATA ARCHIVING STATEMENT

Data for this study are available in the Dryad Digital Repository: https://doi.org/10.5061/dryad.8gtht76sp. This is Paleobiology Database official publication number 496.

Editor. Mary Silcox

SUPPORTING INFORMATION

Additional Supporting Information can be found online (https://doi.org/10.1111/pala.12720):

Appendix S1. Supplementary Methods, Supplementary Figures, and phylogenetic tree in the Newick format.
Appendix S2. Copyright information for Phylopic silhouettes used in Figures 2, 4, 5.

REFERENCES

Adams, D. C. and Collyer, M. L. 2018. Phylogenetic ANOVA: group-clade aggregation, biological challenges, and a refined permutation procedure. *Evolution*, **72**, 1204–1215.

Álvarez-Carretero, S., Tamuri, A. U., Battini, M., Nascimento, F. F., Carlisle, E., Asher, R. J., Yang, Z., Donoghue, P. C. and Dos Reis, M. 2021. A species-level timeline of mammal evolution integrating phylogenomic data. *Nature*, **602**, 1–8.

Archibald, J. D. 2011. *Extinction and radiation: How the fall of dinosaurs led to the rise of mammals*. Johns Hopkins University Press.

Barr, W. A. and Scott, R. S. 2014. Phylogenetic comparative methods complement discriminant function analysis in ecomorphology. *American Journal of Physical Anthropology*, **153**, 663–674.

Benevento, G. L., Benson, R. B. and Friedman, M. 2019. Patterns of mammalian jaw ecomorphological disparity during the Mesozoic/Cenozoic transition. *Proceedings of the Royal Society B*, **286**, 20190347.

Benton, M. J. 1983. Macroevolution: large-scale replacements in the history of life. *Nature*, **302**, 16–17.

Benton, M. J. 1987. Progress and competition in macroevolution. *Biological Reviews*, **62**, 305–338.

Benton, M. J. 2009. The Red Queen and the Court Jester: species diversity and the role of biotic and abiotic factors through time. *Science*, **323**, 728–732.

Brocklehurst, N. 2017. Rates of morphological evolution in Captorhinidae: an adaptive radiation of Permian herbivores. *PeerJ*, **5**, e3200.

Brusatte, S. L., Benton, M. J., Ruta, M. and Lloyd, G. T. 2008. The first 50 Myr of dinosaur evolution: macroevolutionary pattern and morphological disparity. *Biology Letters*, **4**, 733–736.

Brusatte, S. L., Montanari, S., Yi, H.-Y. and Norell, M. A. 2011. Phylogenetic corrections for morphological disparity analysis: new methodology and case studies. *Paleobiology*, **37**, 1–22.

Butler, M. A. and King, A. A. 2004. Phylogenetic comparative analysis: a modeling approach for adaptive evolution. *The American Naturalist*, **164**, 683–695.

Cantalapiedra, J. L., Prado, J. L., Fernández, M. H. and Alberdi, M. T. 2017. Decoupled ecomorphological evolution and diversification in Neogene-Quaternary horses. *Science*, **355**, 627–630.

Carbone, C., Mace, G. M., Roberts, S. C. and Macdonald, D. W. 1999. Energetic constraints on the diet of terrestrial carnivores. *Nature*, **402**, 286–288.

Carbone, C., Teacher, A. and Rowcliffe, J. M. 2007. The costs of carnivory. *PLoS Biology*, **5**, e22.

Carrano, M. 1999. What, if anything, is a cursor? Categories versus continua for determining locomotor habit in mammals and dinosaurs. *Journal of Zoology*, **247**, 29–42.

Carrizo, L. V., Tulli, M. J., Dos Santos, D. A. and Abdala, V. 2014. Interplay between postcranial morphology and locomotor types in Neotropical sigmodontine rodents. *Journal of Anatomy*, **224**, 469–481.

Castiglione, S., Serio, C., Mondanaro, A., Melchionna, M. and Raia, P. 2022. Fast production of large, time-calibrated, informal supertrees with tree.merger. *Palaeontology*, **65**, e12588.

Cerdeño, E. 1996. Rhinocerotidae from the Middle Miocene of the Tung-gur Formation, Inner Mongolia (China). *American Museum Novitates*, **3184**, 1–43.

Chen, M. and Wilson, G. P. 2015. A multivariate approach to infer locomotor modes in Mesozoic mammals. *Paleobiology*, **41**, 280–312.

Christiansen, P. 2002. Locomotion in terrestrial mammals: the influence of body mass, limb length and bone proportions on speed. *Zoological Journal of the Linnean Society*, **136**, 685–714.

Christison, B. E., Gaidies, F., Pineda-Munoz, S., Evans, A. R., Gilbert, M. A. and Fraser, D. 2022. Dietary niches of creodonts and carnivorans of the late Eocene Cypress Hills Formation. *Journal of Mammalogy*, **103**, 2–17.

Clauss, M., Nurutdinova, I., Meloro, C., Gunga, H. C., Jiang, D., Koller, J., Herkner, B., Sander, P. M. and Hellwich, O. 2017. Reconstruction of body cavity volume in terrestrial tetrapods. *Journal of Anatomy*, **230**, 325–336.

Clauss, M., Müller, D. W. and Codron, D. 2019. Within-niche pace of life acceleration as a fundamental evolutionary principle: a mammal pilot test case. *Evolutionary Ecology Research*, **20**, 385–401.

Clauss, M., Codron, D. and Hummel, J. 2023. Equid nutritional physiology and behavior: an evolutionary perspective. *Journal of Equine Veterinary Science*, **124**, 104265.

Clemens, W. A. 2002. Evolution of the mammalian fauna across the Cretaceous-Tertiary boundary in northeastern Montana and other areas of the Western Interior. *In* Hartman, J. H., Johnson, K. R. and Nichols, D. J. (eds) *The Hell Creek Formation and the Cretaceous-Tertiary boundary in the northern Great Plains: An integrated continental record of the end of the Cretaceous*. Geological Society of America, Special Papers, **361**.

Cohen, K. M., Finney, S. C., Gibbard, P. L. and Fan, J.-X. 2013. updated. The ICS international chronostratigraphic chart. *Episodes*, **36**, 199–204. https://stratigraphy.org/ICSchart/ChronostratChart2021-07.pdf

Collyer, M. L. and Adams, D. C. 2020. Phylogenetically aligned component analysis. *Methods in Ecology & Evolution*, **12**, 359–372.

Cross, S. R., Moon, B. C., Stubbs, T. L., Rayfield, E. J. and Benton, M. J. 2022. Climate, competition, and the rise of mosasauroid ecomorphological disparity. *Palaeontology*, **65**, e12590.

Damuth, J. D. and MacFadden, B. J. 1990. *Body size in mammalian paleobiology: Estimation and biological implications*. Cambridge University Press.

De Cuyper, A., Clauss, M., Carbone, C., Codron, D., Cools, A., Hesta, M. and Janssens, G. P. 2019. Predator size and prey size–gut capacity ratios determine kill frequency and carcass production in terrestrial carnivorous mammals. *Oikos*, **128**, 13–22.

Elton, S. 2001. Locomotor and habitat classifications of cercopithecoid postcranial material from Sterkfontein Member 4, Bolt's Farm and Swartkrans Members 1 and 2, South Africa. *Palaeontologia Africana*, **37**, 115–126.

Elton, S. 2002. A reappraisal of the locomotion and habitat preference of *Theropithecus oswaldi*. *Folia Primatologica*, **73**, 252–280.

Elton, S. 2006. 40 years on and still going strong: the use of the hominin-cercopithecid comparison in human evolution. *Journal of the Royal Anthropological Institute*, **12**, 19–38.

Elton, S., Jansson, A. U., Meloro, C., Louys, J., Plummer, T. and Bishop, L. C. 2016. Exploring morphological generality in the Old World monkey postcranium using an ecomorphological framework. *Journal of Anatomy*, **228**, 534–560.

Estes, R. D. 1974. Social organization of the African Bovidae. 166–205. *In* Geist, V. and Walther, E. (eds) *The behaviour of ungulates and its relation to management*. International Union for Conservation of Nature & Natural Resources, Morges, Switzerland.

Etienne, C., Filippo, A., Cornette, R. and Houssaye, A. 2021. Effect of mass and habitat on the shape of limb long bones: a morpho-functional investigation on Bovidae (Mammalia: Cetartiodactyla). *Journal of Anatomy*, **238**, 886–904.

Felsenstein, J. 1973. Maximum-likelihood estimation of evolutionary trees from continuous characters. *American Journal of Human Genetics*, **25**, 471.

Felsenstein, J. 1985. Phylogenies and the comparative method. *The American Naturalist*, **125**, 1–15.

Felsenstein, J. 2012. A comparative method for both discrete and continuous characters using the threshold model. *The American Naturalist*, **179**, 145–156.

Ferretti, F., Lovari, S., Lucherini, M., Hayward, M. and Stephens, P. A. 2020. Only the largest terrestrial carnivores increase their dietary breadth with increasing prey richness. *Mammal Review*, **50**, 291–303.

Figueirido, B., Pérez-Claros, J. A., Torregrosa, V., Martín-Serra, A. and Palmqvist, P. 2010. Demythologizing *Arctodus simus*, the 'short-faced'long-legged and predaceous bear that never was. *Journal of Vertebrate Paleontology*, **30**, 262–275.

Figueirido, B., Martín-Serra, A., Tseng, Z. and Janis, C. 2015. Habitat changes and changing predatory habits in North American fossil canids. *Nature Communications*, **6**, 1–11.

Figueirido, B., Palmqvist, P., Pérez-Claros, J. A. and Janis, C. M. 2019. Sixty-six million years along the road of mammalian ecomorphological specialization. *Proceedings of the National Academy of Sciences*, **116**, 12698–12703.

Florko, K. R., Thiemann, G. W., Bromaghin, J. F. and Richardson, E. S. 2021. Diet composition and body condition of polar bears (*Ursus maritimus*) in relation to sea ice habitat in the Canadian High Arctic. *Polar Biology*, **44**, 1445–1456.

Flynn, J., Janis, C., Scott, K. and Jacobs, L. 1998. Early Cenozoic Carnivora ("Miacoidea"). 110–123. *In* Janis, C. M., Scott, K. M. and Jacobs, L. L. (eds) *Evolution of Tertiary mammals of North America. Vol. 1*. Cambridge University Press.

Flynn, J., Finarelli, J. and Spaulding, M. 2010. Phylogeny of the Carnivora and Carnivoramorpha, and the use of the fossil record to enhance understanding of evolutionary transformations. 25–63. *In* Goswami, A. and Friscia, A. (eds) *Carnivoran evolution: New views on phylogeny, form, and function*. Cambridge University Press.

Foote, M. 1993. Contributions of individual taxa to overall morphological disparity. *Paleobiology*, **19**, 403–419.

Foote, M. 1997. The evolution of morphological diversity. *Annual Review of Ecology & Systematics*, **28**, 129–152.

Friscia, A. R. and Van Valkenburgh, B. 2010. Ecomorphology of North American Eocene carnivores: evidence for competition between carnivorans and creodonts. 311–341. *In* Goswami, A. and Friscia, A. (eds) *Carnivoran evolution: New views on phylogeny, form and function*. Cambridge University Press.

Garland, T. 1983. The relation between maximal running speed and body mass in terrestrial mammals. *Journal of Zoology*, **199**, 157–170.

Garland, T. and Janis, C. M. 1993. Does metatarsal/femur ratio predict maximal running speed in cursorial mammals? *Journal of Zoology*, **229**, 133–151.

Gingerich, P. D. 2006. Environment and evolution through the Paleocene–Eocene thermal maximum. *Trends in Ecology & Evolution*, **21**, 246–253.

Goswami, A. and Friscia, A. 2010. *Carnivoran evolution: New views on phylogeny, form and function*. Cambridge University Press.

Gould, F. D. 2017. Testing the role of cursorial specializations as adaptive key innovations in Paleocene-Eocene ungulates of North America. *Journal of Mammalian Evolution*, **24**, 453–463.

Grossnickle, D. M., Smith, S. M. and Wilson, G. P. 2019. Untangling the multiple ecological radiations of early mammals. *Trends in Ecology & Evolution*, **34**, 936–949.

Guillerme, T. 2018. dispRity: a modular R package for measuring disparity. *Methods in Ecology & Evolution*, **9**, 1755–1763.

Guillerme, T., Cooper, N., Brusatte, S. L., Davis, K. E., Jackson, A. L., Gerber, S., Goswami, A., Healy, K., Hopkins, M. J. and Jones, M. E. 2020. Disparities in the analysis of morphological disparity. *Biology Letters*, **16**, 20200199.

Harmon, L. J., Losos, J. B., Jonathan Davies, T., Gillespie, R. G., Gittleman, J. L., Bryan Jennings, W., Kozak, K. H., McPeek, M. A., Moreno-Roark, F. and Near, T. J. 2010. Early bursts of body size and shape evolution are rare in comparative data. *Evolution*, **64**, 2385–2396.

Harris, M. A. and Steudel, K. 1997. Ecological correlates of hind-limb length in the Carnivora. *Journal of Zoology*, **241**, 381–408.

Hoeks, S., Huijbregts, M. A., Busana, M., Harfoot, M. B., Svenning, J. C. and Santini, L. 2020. Mechanistic insights into the role of large carnivores for ecosystem structure and functioning. *Ecography*, **43**, 1752–1763.

Hopkins, M. J. and Gerber, S. 2021. Morphological disparity. 965–976. *In* Nuño De La Rosa, L. and Müller, G. B. (eds) *Evolutionary developmental biology: A reference guide*. Springer.

Iversen, M., Aars, J., Haug, T., Alsos, I. G., Lydersen, C., Bachmann, L. and Kovacs, K. M. 2013. The diet of polar bears (*Ursus maritimus*) from Svalbard, Norway, inferred from scat analysis. *Polar Biology*, **36**, 561–571.

Janis, C. M. 1989. A climatic explanation for patterns of evolutionary diversity in ungulate mammals. *Palaeontology*, **32**, 463–481.

Janis, C. 2008. An evolutionary history of browsing and grazing ungulates. 21–45. *In* Gordon, I. J. and Prins, H. H. T. (eds) *The ecology of browsing and grazing*. Springer.

Janis, C. M. and Wilhelm, P. B. 1993. Were there mammalian pursuit predators in the Tertiary? Dances with wolf avatars. *Journal of Mammalian Evolution*, **1**, 103–125.

Kielan-Jaworowska, Z., Cifelli, R. L. and Luo, Z.-X. 2004. *Mammals from the age of dinosaurs: Origins, evolution, and structure*. Columbia University Press.

Lamsdell, J. C. and Selden, P. A. 2017. From success to persistence: identifying an evolutionary regime shift in the diverse Paleozoic aquatic arthropod group Eurypterida, driven by the Devonian biotic crisis. *Evolution*, **71**, 95–110.

Levering, D., Hopkins, S. and Davis, E. 2017. Increasing locomotor efficiency among North American ungulates across the Oligocene-Miocene boundary. *Palaeogeography, Palaeoclimatology, Palaeoecology*, **466**, 279–286.

Lidgard, S., Di Martino, E., Zágoršek, K. and Liow, L. H. 2021. When fossil clades 'compete': local dominance, global diversification dynamics and causation. *Proceedings of the Royal Society B*, **288**, 20211632.

Lovegrove, B. G. 2004. Locomotor mode, maximum running speed, and basal metabolic rate in placental mammals. *Physiological & Biochemical Zoology*, **77**, 916–928.

Lovegrove, B. G. and Haines, L. 2004. The evolution of placental mammal body sizes: evolutionary history, form, and function. *Oecologia*, **138**, 13–27.

Lovegrove, B. and Mowoe, M. 2013. The evolution of mammal body sizes: responses to Cenozoic climate change in North American mammals. *Journal of Evolutionary Biology*, **26**, 1317–1329.

Martín-Serra, A., Figueirido, B. and Palmqvist, P. 2016. In the pursuit of the predatory behavior of Borophagines (Mammalia, Carnivora, Canidae): inferences from forelimb morphology. *Journal of Mammalian Evolution*, **23**, 237–249.

Meachen, J. A., Dunn, R. H. and Werdelin, L. 2016. Carnivoran postcranial adaptations and their relationships to climate. *Ecography*, **39**, 553–560.

Meloro, C. 2011a. Feeding habits of Plio-Pleistocene large carnivores as revealed by the mandibular geometry. *Journal of Vertebrate Paleontology*, **31**, 428–446.

Meloro, C. 2011b. Locomotor adaptations in Plio-Pleistocene large carnivores from the Italian Peninsula: palaeoecological implications. *Current Zoology*, **57**, 269–283.

Meloro, C. and Clauss, M. 2012. Predator-prey biomass fluctuations in the Plio-Pleistocene. *Palaios*, **27**, 90–96.

Meloro, C. and Raia, P. 2010. Cats and dogs down the tree: the tempo and mode of evolution in the lower carnassial of fossil and living Carnivora. *Evolutionary Biology*, **37**, 177–186.

Meloro, C., Raia, P. and Barbera, C. 2007. Effect of predation on prey abundance and survival in Plio-Pleistocene mammalian communities. *Evolutionary Ecology Research*, **9**, 505–525.

Mihlbachler, M. C. and Solounias, N. 2006. Coevolution of tooth crown height and diet in oreodonts (Merycoidodontidae, Artiodactyla) examined with phylogenetically independent contrasts. *Journal of Mammalian Evolution*, **13**, 11–36.

Morales-García, N. M., Säilä, L. K. and Janis, C. M. 2020. The neogene savannas of North America: A retrospective analysis on artiodactyl faunas. *Frontiers in Earth Science*, **8**, 191.

Morales-García, N. M., Gill, P. G., Janis, C. M. and Rayfield, E. J. 2021. Jaw shape and mechanical advantage are indicative of diet in Mesozoic mammals. *Communications Biology*, **4**, 1–14.

Navarro, N. 2003. MDA: a Matlab-based program for morphospace-disparity analysis. *Computers & Geosciences*, **29**, 655–664.

Nyakatura, K. and Bininda-Emonds, O. R. 2012. Updating the evolutionary history of Carnivora (Mammalia): a new species-level supertree complete with divergence time estimates. *BMC Biology*, **10**, 12.

Oksendal, B. 2013. *Stochastic differential equations: An introduction with applications*. Springer Science & Business Media.

Orme, D., Freckleton, R., Thomas, G., Petzoldt, T., Fritz, S., Issac, N. and Pearse, W. 2018. caper: comparative analysis of phylogenetics and evolution in R. Version 1.0. 1. https://cran.r-project.org/web/packages/caper/index.html

Osborn, H. F. 1902. The law of adaptive radiation. *The American Naturalist*, **36**, 353–363.

Owen-Smith, R. 1988. *Megaherbivores: The influence of very large body size on ecology*. Cambridge University Press.

Owen-Smith, N. and Mills, M. G. 2008. Predator–prey size relationships in an African large-mammal food web. *Journal of Animal Ecology*, **77**, 173–183.

Pagel, M. 1999. Inferring the historical patterns of biological evolution. *Nature*, **401**, 877–884.

Paradis, E. and Schliep, K. 2019. ape 5.0: an environment for modern phylogenetics and evolutionary analyses in R. *Bioinformatics*, **35**, 526–528.

Pennell, M. W., Eastman, J. M., Slater, G. J., Brown, J. W., Uyeda, J. C., Fitzjohn, R. G., Alfaro, M. E. and Harmon, L. J. 2014. geiger v2.0: an expanded suite of methods for fitting macroevolutionary models to phylogenetic trees. *Bioinformatics*, **30**, 2216–2218.

Penteriani, V. and Melletti, M. 2020. *Bears of the world: Ecology, conservation and management*. Cambridge University Press.

Polly, P. D. 2007. Limbs in mammalian evolution. 245–268. *In* Hall, B. K. (ed.) *Fins into limbs: Evolution, development and transformation*. University of Chicago Press.

Pontzer, H. and Kamilar, J. M. 2009. Great ranging associated with greater reproductive investment in mammals. *Proceedings of the National Academy of Sciences*, **106**, 192–196.

Prentice, K. C., Ruta, M. and Benton, M. J. 2011. Evolution of morphological disparity in pterosaurs. *Journal of Systematic Palaeontology*, **9**, 337–353.

Raia, P., Castiglione, S., Serio, C., Mondanaro, A., Melchionna, M. and Di Febbraro, M. 2019. RRphylo: Phylogenetic Ridge Regression Methods for Comparative Studies. R package version 2. https://rdrr.io/cran/RRphylo/man/RRphylo-package.html

R Core Team. 2023. R: A Language and Environment for Statistical Computing. R Foundation for Statistical Computing. Vienna, Austria.

Reeves, J. C., Moon, B. C., Benton, M. J. and Stubbs, T. L. 2021. Evolution of ecospace occupancy by Mesozoic marine tetrapods. *Palaeontology*, **64**, 31–49.

Reitan, T. and Liow, L. H. 2019. Layeranalyzer: inferring correlative and causal connections from time series data in R. *Methods in Ecology & Evolution*, **10**, 2183–2188.

Revell, L. J. 2009. Size-correction and principal components for interspecific comparative studies. *Evolution: International Journal of Organic Evolution*, **63**, 3258–3268.

Revell, L. J. 2010. Phylogenetic signal and linear regression on species data. *Methods in Ecology & Evolution*, **1**, 319–329.

Revell, L. J. 2012. phytools: an R package for phylogenetic comparative biology (and other things). *Methods in Ecology & Evolution*, **3**, 217–223.

Roka, B., Jha, A. K. and Chhetri, D. R. 2021. A study on plant preferences of red panda (*Ailurus fulgens*) in the wild habitat: foundation for the conservation of the species. *Acta Biologica Sibirica*, **7**, 425.

Ruta, M., Angielczyk, K. D., Fröbisch, J. and Benton, M. J. 2013. Decoupling of morphological disparity and taxic diversity during the adaptive radiation of anomodont therapsids. *Proceedings of the Royal Society B*, **280**, 20131071.

Saarinen, J., Mantzouka, D. and Sakala, J. 2020. Aridity, cooling, open vegetation, and the evolution of plants and animals during the Cenozoic. 83–107. *In* Martinetto, E., Tschopp, E. and Gastaldo, R. A. (eds) *Nature through time: Virtual field trips through the nature of the past*. Springer.

Schaeffer, J., Benton, M. J., Rayfield, E. J. and Stubbs, T. L. 2020. Morphological disparity in theropod jaws: comparing discrete characters and geometric morphometrics. *Palaeontology*, **63**, 283–299.

Schellhorn, R. and Pfretzschner, H.-U. 2015. Analyzing ungulate long bones as a tool for habitat reconstruction. *Mammal Research*, **60**, 195–205.

Sepkoski, J. J. Jr. 1996. Competition in macroevolution: the double wedge revisited. 211–255. *In* Jablonski, D., Erwin, D.H. and Lipps, J.H. (eds) *Evolutionary paleobiology*. Chicago University Press.

Serio, C., Raia, P. and Meloro, C. 2020. Locomotory adaptations in 3D humerus geometry of Xenarthra: testing for convergence. *Frontiers in Ecology & Evolution*, **8**, 139.

Serio, C., Brown, R., Clauss, M. and Meloro, C. 2024. Data from: Morphological disparity of mammalian limb bones throughout the Cenozoic: the role of biotic and abiotic factors. [dataset]. Dryad. https://doi.org/10.5061/dryad.8gtht76sp

Shelley, S. L., Brusatte, S. L. and Williamson, T. E. 2021. Quantitative assessment of tarsal morphology illuminates locomotor behaviour in Palaeocene mammals following the end-Cretaceous mass extinction. *Proceedings of the Royal Society B*, **288**, 20210393.

Simpson, G. G. 1944. *Tempo and mode in evolution*. Columbia University Press.

Slater, G. J. 2013. Phylogenetic evidence for a shift in the mode of mammalian body size evolution at the Cretaceous-Palaeogene boundary. *Methods in Ecology & Evolution*, **4**, 734–744.

Stubbs, T. L., Pierce, S. E., Elsler, A., Anderson, P. S., Rayfield, E. J. and Benton, M. J. 2021. Ecological opportunity and the rise and fall of crocodylomorph evolutionary innovation. *Proceedings of the Royal Society B*, **288**, 20210069.

Sunquist, M. E. and Sunquist, F. C. 1989. Ecological constraints on predation by large felids. 283–301. *In* Gittleman, J. L. (ed.) *Carnivore behavior, ecology, and evolution*. Springer.

Toledo, N., Muñoz, N. A. and Cassini, G. H. 2021. Ulna of extant xenarthrans: shape, size, and function. *Journal of Mammalian Evolution*, **28**, 35–45.

Van Valkenburgh, B. 1999. Major patterns in the history of carnivorous mammals. *Annual Review of Earth & Planetary Sciences*, **27**, 463–493.

Van Valkenburgh, B. 2007. Déjà vu: the evolution of feeding morphologies in the Carnivora. *Integrative & Comparative Biology*, **47**, 147–163.

Wesley-Hunt, G. D. 2005. The morphological diversification of carnivores in North America. *Paleobiology*, **31**, 35–55.

Wilberg, E. W. 2017. Investigating patterns of crocodyliform cranial disparity through the Mesozoic and Cenozoic. *Zoological Journal of the Linnean Society*, **181**, 189–208.

Yang, Z. 2006. *Computational molecular evolution*. Oxford Universitiy Press.

Zachos, J. C., Dickens, G. R. and Zeebe, R. E. 2008. An early Cenozoic perspective on greenhouse warming and carbon-cycle dynamics. *Nature*, **451**, 279–283.

Zack, S. P. 2019. A skeleton of a Uintan machaeroidine 'creodont'and the phylogeny of carnivorous eutherian mammals. *Journal of Systematic Palaeontology*, **17**, 653–689.

Zimicz, N. 2014. Avoiding competition: the ecological history of late Cenozoic metatherian carnivores in South America. *Journal of Mammalian Evolution*, **21**, 383–393.

Zurano, J. P., Magalhães, F. M., Asato, A. E., Silva, G., Bidau, C. J., Mesquita, D. O. and Costa, G. C. 2019. Cetartiodactyla: updating a time-calibrated molecular phylogeny. *Molecular Phylogenetics & Evolution*, **133**, 256–262.